CHEMPHYSCHEM

DOI: 10.1002/cphc.201000866

# How Förster Resonance Energy Transfer Imaging Improves the Understanding of Protein Interaction Networks in Cancer Biology

Gilbert O. Fruhwirth,*[a, f] Luis P. Fernandes,[b] Gregory Weitsman,[a] Gargi Patel,[a] Muireann Kelleher,[a] Katherine Lawler,[f] Adrian Brock,[a] Simon P. Poland,[f] Daniel R. Matthews,[a] Gergely Keri,[c] Paul R. Barber,[d] Borivoj Vojnovic,[b, d] Simon M. Ameer-Beg,[a, b] Anthony C. C. Coolen,[b, e] Franca Fraternali,[b] and Tony Ng*[a, b, f]

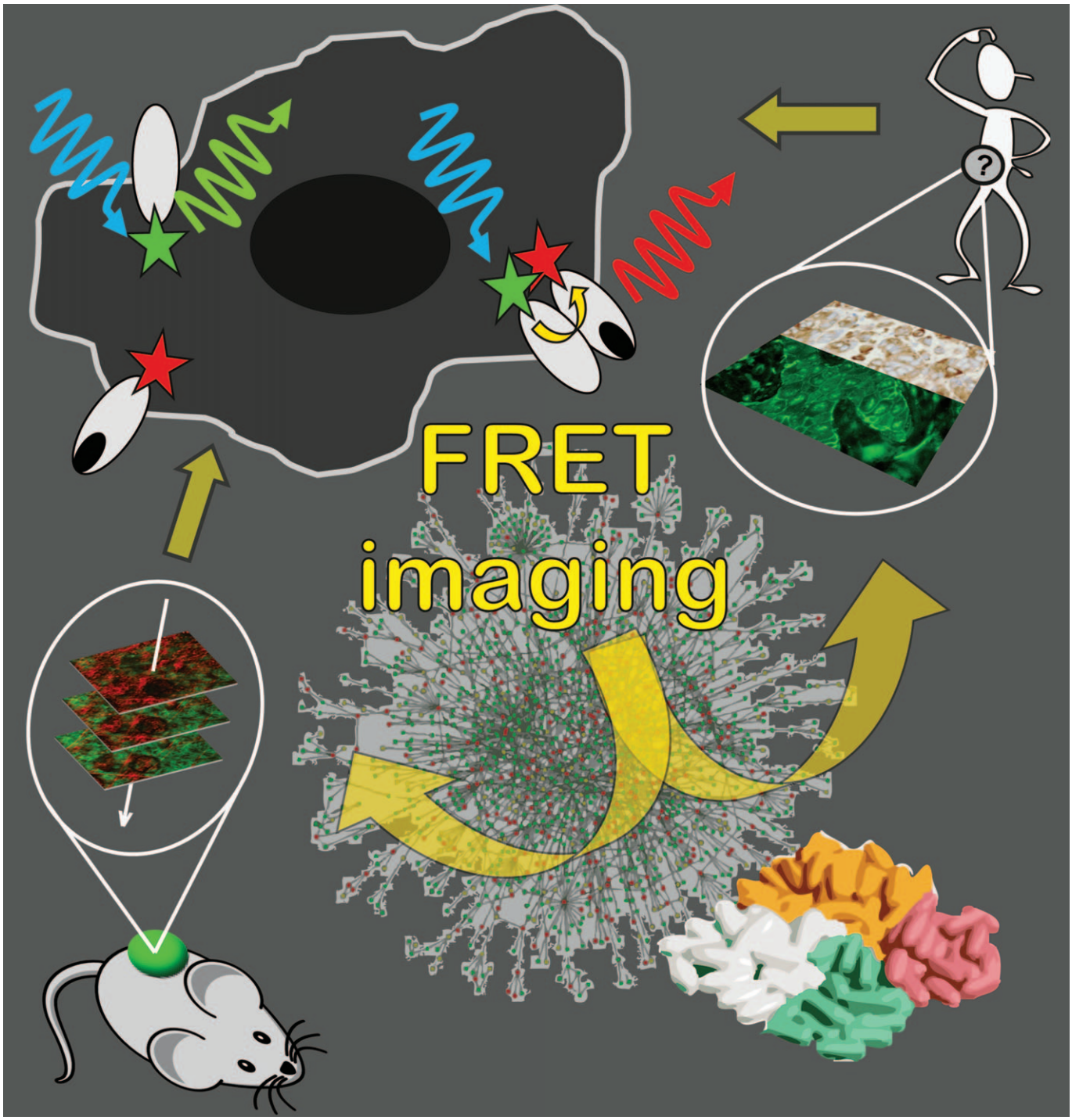

Herein we discuss how FRET imaging can contribute at various stages to delineate the function of the proteome. Therefore, we briefly describe FRET imaging techniques, the selection of suitable FRET pairs and potential caveats. Furthermore, we discuss state-of-the-art FRET-based screening approaches (underpinned by protein interaction network analysis using computational biology) and preclinical intravital FRET-imaging techniques that can be used for functional validation of candidate hits (nodes and edges) from the network screen, as well as measurement of the efficacy of perturbing these nodes/edges by short hairpin RNA (shRNA) and/or small molecule-based approaches.

## 1. Overview

Molecular imaging plays a crucial role in our quest to translate the knowledge of the cancer genome/proteome to potential clinical benefits by, for instance, monitoring spatiotemporally the molecular and cell biological (pharmacodynamic) response to anti-tumour therapeutics (Figure 1). A multi-scale imaging approach is required to tackle the genome-wide scale of gene/protein network complexity, thereby requiring high content/throughput imaging in order to understand cancer proteome sensitivity and more specifically, to identify the so-called fragile points (individual proteins or specific protein–protein interactions) within the proteome which can be targeted efficiently.[1] In Section 2 we provide a brief review of the current FRET technologies including considerations regarding the selection of appropriate fluorophores and in Section 3 we discuss high-content adaptations of some of these technologies.

The high-content image datasets can be further analysed by using the existing protein interaction bioinformatics tools that serve as a platform to provide a filter for the initial hits and/or to organise these hits into functional modules. Some of these current bioinformatics approaches and our own recent approach to use this platform to design targeted siRNA screens are described in Section 4.

Once the crucial target protein interactions are identified from the high-content screen, monitoring the pharmacodynamic responses to anti-tumour therapeutics requires mapping the spatially heterogeneous protein proximity (measured in nanometer scale) within tumour cells, in vivo, at the whole body level. This also implies a prerequisite requirement for multiple imaging modalities, since a combination of image resolution, depth as well as temporal resolution is necessary.[2] Hence, we briefly discuss current in vivo FRET imaging techniques and then focus on new developments in microscopic intravital FRET imaging (Section 5).

In terms of clinical practice, we aim to eventually apply the tools and knowledge, accumulated through the aforementioned bioinformatics-driven high content imaging approaches, to benefit our assessment of the signalling protein network organisation in excised and/or biopsied cancer tissues. Although much of this endeavour lies outside the scope of this article, an outlook perspective is provided in the final section entitled "Towards systems pathology".

### 1.1. Why FRET Imaging for Protein–Protein Interactions?

The complete information every organism needs for life is encrypted in its genome. For instance, the human genome encodes an estimated 21 000 different genes containing instructions on how to make proteins. Technological and bioinformatical advancements within the past decade, together with the increased use of the vast amounts of biological and chemical data already available, have made possible the construction of gene/protein networks that are responsible for various cellular functions, using computational approaches. The commonly used biochemical genomic approach to provide input data, at a proteome-wide level for mapping these networks, involves protein extraction from cells, followed by one- or two-dimensional (2D) gel electrophoresis coupled with mass spectrometry (MS).[3] Shotgun methods provide useful alternatives to gels, whereby proteins are first digested into more complex peptide mixtures that are then analysed directly by liquid chromatography coupled to MS. The hydrophobic nature of cell membrane proteins makes them difficult to extract by digestion, keeping them under-represented in proteomic analyses, despite the fact these provide the majority of the "biosensors" within the

[a] *Dr. G. O. Fruhwirth, Dr. G. Weitsman, Dr. G. Patel, Dr. M. Kelleher, A. Brock, Dr. D. R. Matthews, Dr. S. M. Ameer-Beg, Prof. T. Ng*
*Richard Dimbleby Department of Cancer Research*
*Division of Cancer Studies*
*King's College London*
*Guy's Medical School Campus, NHH, SE1 1UL (UK)*
*Fax: (+44) (0) 20 7848 6220*
*Fax: (+44) (0) 20 7848 8056*
*E-mail: gilbert.fruhwirth@kcl.ac.uk*
*tony.ng@kcl.ac.uk*

[b] *Dr. L. P. Fernandes, Prof. B. Vojnovic, Dr. S. M. Ameer-Beg, Prof. A. C. C. Coolen, Dr. F. Fraternali, Prof. T. Ng*
*Randall Division of Cell & Molecular Biophysics*
*King's College London*
*Guy's Medical School Campus, NHH, SE1 1UL (UK)*

[c] *Prof. G. Keri*
*Vichem Chemie Research Ltd.*
*Herman Ottó utca 15, Budapest, Hungary and*
*Pathobiochemistry Research Group of Hungarian Academy of Science*
*Semmelweis University, Budapest, 1444 Bp 8. POB 260 (Hungary)*

[d] *Dr. P. R. Barber, Prof. B. Vojnovic*
*Gray Institute for Radiation Oncology & Biology*
*University of Oxford*
*Old Road Campus Research Building*
*Roosevelt Drive, Oxford, OX3 7DQ (UK)*

[e] *Prof. A. C. C. Coolen*
*Department of Mathematics*
*King's College London*
*Strand Campus, London, WC2R 2LS (UK)*

[f] *Dr. G. O. Fruhwirth, Dr. K. Lawler, Dr. S. P. Poland, Prof. T. Ng*
*Comprehensive Cancer Imaging Centre*
*New Hunt's House, Guy's Medical School Campus, NHH, SE1 1UL (UK)*

Supporting information for this article is available on the WWW under http://dx.doi.org/10.1002/cphc.201000866.

  

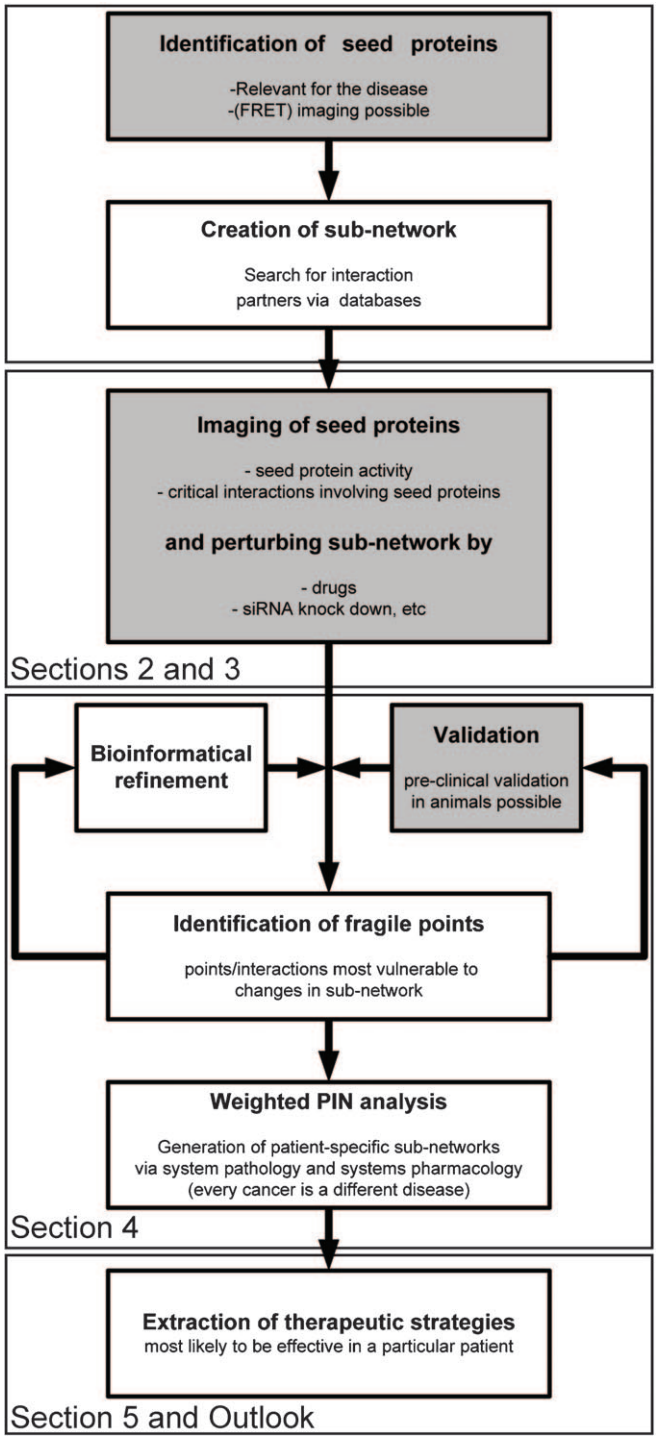


**Figure 1.** Outline for the generation of a protein interaction network. Scheme for the use of protein interaction subnetworks as a means towards personalized medicine. Steps in which FRET imaging of protein–protein interactions or biosensor molecules can report valuable information are shaded in gray. The boxes refer to individual chapters of this review and capital letters refer to the respective sections.

human genome. Detection sensitivity is influenced by the affinity of interactions, abundance of protein partners, and whether the association is direct or through intermediate binding partners. All these methods provide us with snaphots of the proteome landscape under different conditions and perturbations, and of the complex cross-talk of the components. Our interpretation of this landscape in terms of the underlying biological processes is limited by the different nature of the methodological biases and by the availability of rigorous measures to quantify these. One possibility is to use information-theory to analyse the macroscopic nature of the different proteomic snapshots and to extract consistent topological properties.[4]

Various imaging-based high content/throughput screening approaches have recently been tested in different cell biological contexts.[5–8] Together with the recently described, automated FRET approaches,[9–11] these imaging approaches present certain advantages over incumbent technologies. First, the post-translational protein modifications or protein complexes are better preserved and directly observed in situ. Second, the sensitivity of detecting membrane events is enhanced, compared to biochemical extraction of membrane complexes. Third, these approaches raise the possibility of monitoring the kinetics of various protein events, their timing, and their cellular localisation in situ in a physiologic way. Fourth, to maximise the information content from the data and obtain the so-called system response profiles (SRPs), it is necessary to obtain not only steady-state data, but also to perform negative feedback and feedforward network analysis of the proteomic response to various perturbations.[12] This type of experiment is best performed in intact cells by an imaging approach. Fifth, with an optical approach combined with mathematical analysis, a full functional analysis of the sensitivity[13] within the human interactome in situ can be achieved and subsequently validated.

FRET is a technology relying on non-radiative energy transfer between two molecules in close proximity to measure distance and orientation. Exploitation of FRET imaging has significantly contributed to an improved understanding of molecular interactions involved in physiologic as well as pathophysiologic cellular processes including cell division/growth,[14] cell adhesion/motility/invasion,[15–21] cell senescence/apoptosis,[22] and the underlying signal transduction processes.

## 2. FRET Imaging: Techniques and Selection of Probes

In this section we briefly describe currently available techniques for the determination of FRET in imaging applications and discuss the selection of appropriate donor and acceptor molecules for FRET experiments.

For the quantitative assessment of protein interactions (e.g. as a consequence of cellular stimulation or drug treatment) there are a limited number of techniques available. If that task has to be performed in a spatiotemporally controlled manner in live cells or organisms to retain the dynamic dimension of the experiment then it is even more difficult to obtain the desired information. FRET imaging combines the spatiotemporal information accessible by microscopy with the nanometer-range FRET phenomena and thus can be considered to break the diffraction limit of conventional microscopic techniques. The photophysical phenomenon of non-radiative energy trans-

  

fer via a long-range dipole–dipole coupling from an excited-state donor fluorophore to a ground-state acceptor molecule (Figure 2 A) was first described by Förster fifty years ago.[23–25] This energy transfer process is inversely proportional to the sixth power on the distance of the two interacting molecules (typically in the range of 1–10 nm). It further depends on the spectral overlap between donor emission and acceptor excitation, the relative orientation of the donor absorption and acceptor transition moments, and the refractive index. FRET leads to a decrease in the fluorescence intensity and the fluorescence lifetime of the donor fluorophore. It usually sensitizes fluorescence emission from the acceptor fluorophore (SE).

Gilbert Fruhwirth received his Ph.D. in biochemistry and biotechnology from Graz University of Technology, Austria, in 2005. While holding a university assistant position there he studied the cellular effects of phospholipid oxidation products. In 2006, he moved as a post-doc to the Richard Dimbleby Department at King's College London (KCL) and developed a strong interest in cancer with a special emphasis on membrane receptor biology. He further specialized in the application of FRET-based techniques for the measurement of protein–protein interaction dynamics. Since 2009 he is a senior post-doc at the KCL- and University College London-based Comprehensive Cancer Imaging Centre.

Luis Pera Fernandes received his B.Sc. in Computational Biology, developing a thesis on Intron phase patterns. In 2010, he has completed his Ph.D. in Bioinformatics at the Randall Division of Cell and Molecular Biophysics at King's College London. During his Ph.D. thesis he worked on topological and structural properties Protein Interaction Networks under the supervision of Dr. Franca Fraternali. He is currently a postdoctoral researcher at the same institution, where he continues his work in network biology.

Gregory Weitsman received his Ph.D. in physiology and pharmacology from Tel Aviv University, Israel, in 2004. The combined knowledge of molecular endocrinology of breast cancer (nuclear receptors biology) and programmed cell death (receptor-activated apoptosis) gained during his Ph.D. was enriched during post-doctoral training in the Univerisity of Manitoba, Canada. Currently, as a research associate at the Richard Dimbleby Department at King's College London, he focuses on modulation of death receptor signalling by dynamic protein complex formation. Newly discovered protein–protein interactions were used as a platform for screening of the library of chemical compounds using FRET technology.

Gargi Patel, a medical oncologist, completed her undergraduate medical degree at the University of Cambridge with a distinction. She carried out her junior doctor training at Guys and St. Thomas Hospital, amongst other London teaching university hospitals. She interrupted her specialist training in order to carry out a Ph.D. at King's College London, using FRET/FLIM assays in breast cancer, under Prof. Tony Ng. She is in her second year, and recently received the McElwain Fellowship from Cancer Research UK for her research.

Muireann Kelleher is a consultant medical oncologist in St. George's Hospital and Honorary Senior Lecturer in St. George's University of London. She completed her undergraduate medical degree in University College Cork; working in the UK since 2000. Her speciality training took place in Guys, King's and St. Thomas Hospitals. During her 2009 Ph.D. thesis in the Ng laboratory (KCL) she used optical imaging to study protein–protein interactions in archived cancer tissue and correlated this with metastases and clinical outcome for breast cancer patients. She maintains links with the Ng Group, having a particular interest in individualized cancer therapy.

Katherine Lawler studied at the European Bioinformatics Institute (EMBL–EBI) as an EMBL Predoctoral Fellow, receiving her Ph.D. from the University of Cambridge in 2010 for computational work on genome-scale transcriptional regulation of gene expression. She is a post-doc at the KCL- and University College London-based Comprehensive Cancer Imaging Centre, focusing on the analysis of cancer gene expression and protein-protein interaction datasets with the aim of further characterising tumour subtypes and the relation to clinical outcome.

  

### 2.1. Techniques to Measure FRET

Determination of FRET can either be achieved by 1) intensity-based techniques (ratiometric, or involving SE only), or by the measurement of 2) anisotropy, or 3) fluorescence lifetimes.

For both intensity-based and anisotropy measurements, it is important to use appropriate excitation and emission filter sets, to acquire images at appropriate signal-to-noise ratio levels,[26] and to ensure, by suitable fluorphore selection, that there is no significant cross-excitation of the acceptor when exciting the donor. Upon inhibition of FRET, for example, by

Adrian Brock received his B.Sc. in General Biology from the University of London subsequently working as a Laboratory Scientific Officer in Dermatology Research at The Royal Free Hospital. He later moved into Cancer Research as a member of the Richard Dimbleby Department initially based at St. Thomas Hospital working in the fields of Radiobiology and DNA Flow Cytometry. In 2005 he relocated to the new Richard Dimbleby Department of Cancer Research based at King's College London under Prof. Tony Ng to assist with studies on chemokine and receptor biology.

After completing his Ph.D. in 2006, Simon Poland has been employed as a post-doctoral researcher at the Institute of Photonics, at Strathclyde where for over 3 years he was deeply involved in a number of optical imaging projects for dental and microscopy applications. This included the development of a system to detect and monitor dental caries, the integration of MEMS for laser scanning endoscopy and the use of adaptive optics to improve signal and resolution in confocal and multiphoton microscopy. Since joining King's College at the start of 2010, Simon has been involved in the development of in-vivo imaging modalities for identifying and evaluating drug interactions in tumours.

Daniel Matthews received his Ph.D. in 2003 at the Department of Physics and Astronomy at Cardiff University where he then worked as a post-doctoral researcher until 2007. Here he worked on the integration of novel photonic devices with lab-on-a-chip technology. He has worked with the Richard Dimbleby department of Cancer Research, King's College London since 2007 developing technology for automated high-content screening microscopy. His current research interests include single-molecule imaging and fluorescence lifetime measurements.

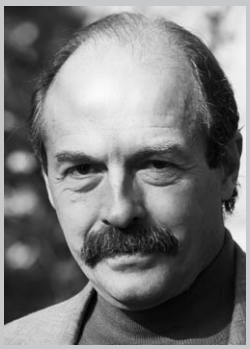

György Kéri is Professor and Head of the Signal Transduction Therapy Laboratory at Semmelweis Universty, and CEO, CSO of Vichem Chemie Research Ltd. He is chemist by profession and got his Ph.D. in biochemistry at Eötvös University, Budapest, and was a post-doc at UCSF Medical Center. He has developed a signal-inhibiting peptide (TT232) which is now in phase II clinical trials, and participated in the development of SU101 (phase III) He was advisor and collaborative partner of SUgen Inc between 1992–1999 and Axxima Pharmaceuticals between 1999 and 2006. He has developed the Nested Chemical LibraryTM Technology, which is a unique technology of lead finding and optimization in the kinase field.

Paul R. Barber graduated from Southampton University, UK, in 1996 with a Ph.D. entitled "Blue laser action in Tm-doped fluoride fibre", after earning a first-class honours degree in Physics with Optoelectronics. During 3 years working for DERA,UK, his interest in image processing grew and in 1999 he joined the Gray Cancer Institute where he applied what he had learnt to problems in biology. Now at the Gray Institute at Oxford University, UK, he enjoys making sophisticated mathematics, algorithms, and microscope systems accessible to the biological community through the programming of computer applications. He has co-authored over 40 papers and lectures at King's and Queen Mary Colleges, University of London.

Borivoj Vojnovic obtained a Ph.D. in radiation physics from the University of London in 1983. Since 1989 he has headed the Advanced Technology Development Group at the Gray Cancer Institute, developing specialised optical imaging methods used in automated cytometry and micro-irradiation. His research interests include the application of advanced optical imaging, image processing and image analysis modalities for tissue and cellular imaging. In 2007, he was appointed Professor of Biophysics Imaging at the University of Oxford.

  

photobleaching the acceptor molecule at its excitation wavelength, the fluorescence intensity and lifetime of the donor should resemble a donor not undergoing FRET. Intensity-based measurements of donor fluorescence and sensitized acceptor emission are widely combined with acceptor photobleaching (APB) to prove specificity of the energy transfer process (SE/APB). SE/APB is by far the most widespread method of measuring FRET, despite several pitfalls. These include 1) dependence of fluorescence intensities on fluorophore concentrations, 2) acceptor cross-excitation, filter bleed-through, 3) contribution of auto-fluorescence to signal levels, 4) the possibility of artefact generation during photobleaching (e.g. increase of fluorescence in the CFP channel upon irradiation of YFP unrelated to FRET[27]), and 5) often low signal-to-noise ratios. This is mainly due to the consequence of using conventional, non-specialized imaging equipment. Alternatively, a ratiometric approach, for example, acceptor emission divided by donor emission, can be recorded in a confocal setup with appropriate filter settings. This ratiometric technique represents a fast way of determining FRET and has been applied frequently in cellular assays.[28–35] It is especially powerful when biosensors are used for the measurement of fast changes in second messenger molecules such as cAMP or calcium in order to measure the cellular response to agonists or antagonists[32,33] or short-lived molecules are of interest.[34] However, as it is an intensity-based method, most of the above mentioned caveats of SE/ABP techniques also have to be considered very carefully and a compromise between fast acquisition speed and quantification accuracy of the measurement has to be reached. The latter is especially important if different cells are compared, but less of an issue if relative FRET dynamics within the same cell are studied.[29] A thorough analysis of the signal-to-noise ratios in intensity-based FRET signals and optimal ways to collect them can be found in ref. [36].

Fluorescence anisotropy is an alternative technique for measuring FRET. The depolarization of sensitized acceptor

Simon Ameer-Beg received his Ph.D. in photochemistry whilst working at British Nuclear Fuels in 1999. Following a postdoctoral position at the Gray Cancer Institute developing multiphoton fluorescence lifetime imaging, he was appointed non-clinical lecturer to the Richard Dimbleby Department of Cancer Research at King's College London in 2006. His research has involved the development of multiphoton in vivo imaging, FLIM, high-content screening and measurement of protein–protein interactions by FRET.

ACC (Ton) Coolen is professor of applied mathematics at King's College London since 2000. He was trained as a theoretical physicist in Utrecht, where he obtained his Ph.D. in 1990 on spin-glass models of neural networks. Before coming to London he spent four years in the group of David Sherrington at the University of Oxford (theoretical physics). His research focuses mainly on the statistical mechanics of disordered many-particle systems in physics, biology and other disciplines. In recent years his main interest has been the development of mathematical methods for biomedical problems, including the analysis of complex cellular signaling networks (proteomic, gene regulatory) and the interaction processes which they support, the extraction of information from biomarker data, and the impact of cohort heterogeneity and competing risks on medical statistics.

Franca Fraternali received her Ph.D. in Physical Chemistry from the University of Naples, working on characterization of protein conformational dynamics by molecular simulations techniques. During her Ph.D. she worked in collaboration with Prof. van Gunsteren at the Polytechnic of Zurich (ETH) and developed implicit solvent models for use in molecular dynamics. She worked as post-doctoral fellow the ETH, at the Institute Le Bel in Strasbourg and at the EMBL in Heidelberg. In 2000 she obtained a staff position in the Mathematical Biology Division of the National Institute for Medical Research in London. Since 2005 she is Reader at King's College within the Randall Division. Her more recent focus is the study of physical interactions of proteins by molecular simulations and bioinformatical and systems biology analyses.

Tony Ng is the Richard Dimbleby Professor of Cancer Research (http://www.dimblebycancercare.org/), King's College London. He has a mix of training/expertise in medicine, immunology, cancer cell biology, biochemistry, optical imaging and cell biophysics. Using FRET and FLIM techniques, his laboratory has established in live and fixed tumour cell systems (including xenografts) imaging-based methods that can monitor post-translational modifications and protein interactions, both in space and time. By combining imaging with bioinformatics and network modelling, his lab is now adopting a multidisciplinary approach to understand the cancer metastatic process and its immunological control.

  

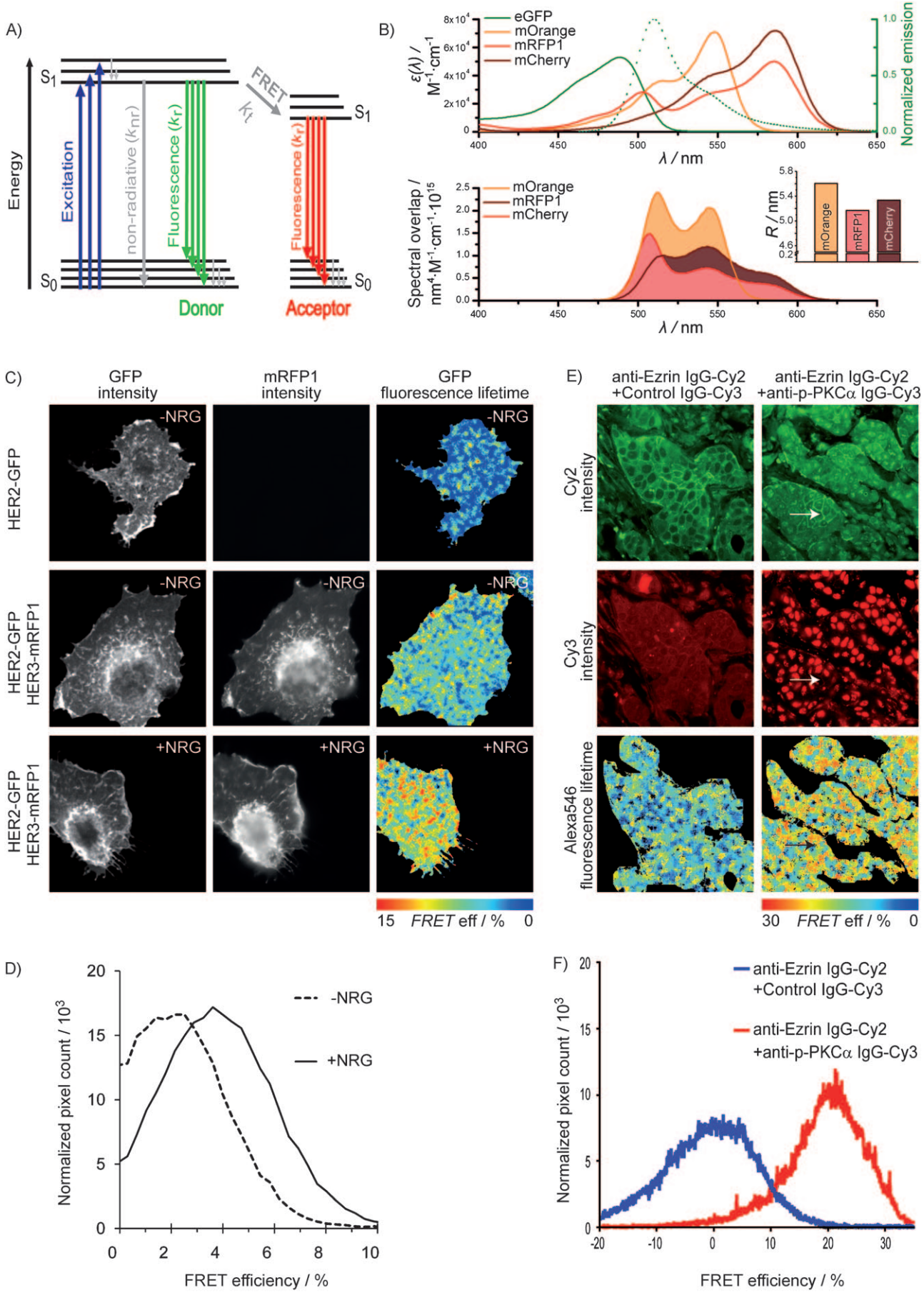


  

emission is measured and visualized as change of fluorescence anisotropy.[9,37] This technique was shown to be applicable in laser scanning and wide-field microscopes, which makes it an excellent candidate for automated high-speed microscopy.[38] The intracellular activities of several FRET-based protein conformation sensing molecules, which we have imaged with fluorescence lifetime imaging microscopy (FLIM), in various cancer biological and immunological contexts,[9,16,39–43] can now be tracked in situ in a fast way and without the difficulty of implementing spectral bleed-through corrections that are normally required in intensity-based steady-state measurements of FRET. Furthermore, the measurement of fluorescence anisotropy also allows the determination of FRET between identical fluorophores. If homo-FRET occurs, the anisotropy decreases, which was used to study protein clustering and to determine cluster sizes with subcellular resolution.[44,45]

FLIM as a means of measuring FRET, has several advantages over intensity-based methods. Firstly, the fluorescence lifetime is independent of the donor fluorophore concentration as long as it is dilute enough[27,46] and, secondly, it is independent of the length of the light path. The gold standard for the determination of FRET by FLIM is by measuring the decrease in donor lifetime.[47,48] Alternatively, the measurement of the delay between an excitation pulse and the onset of the fluorescence lifetime curve of the acceptor has been reported.[49] Fluorescence lifetime measurements can be performed by either time-correlated single photon counting (TCSPC), various time-gating technologies, or frequency domain measurements (FD), all of which have been extensively discussed elsewhere.[50–52] It is not the focus of this article to discuss all the aspects of these techniques. Briefly, FD techniques based on modulated source and detectors are fast as they acquire image information in parallel, rather than pixel-by-pixel, common to laser-scanning methods. However their dynamic range and precision tends to be restricted and their ability to determine multi-exponential decays is limited. Lifetime provides an additional, highly specific contrast mechanism to the imaged sample and the challenge is to use the emitted photons in an efficient manner to derive this contrast. Low and inhomogeneous photon counts plague all FRET methods and more so when FLIM is used. However, the increase in specificity is well worth the application of FLIM, particularly when stoichiometry is unknown or cannot be controlled, for example, when FRET donor and FRET acceptor molecules are on separate proteins. From our own experience with a TD-setup we can readily detect a 75 ps change in a 2.2 ns fluorescence lifetime. This is equivalent to a 3% change in FRET efficiency [Eq. (1)], in which $\tau_D$ is defined as the unquenched donor fluorescence lifetime and $\tau$ is the fluorescence lifetime when FRET is occurring.

$$\text{FRET efficiency} = \frac{\tau_D - \tau}{\tau_D} \quad (1)$$

This level of accuracy can be corroborated by published accounts of theoretical and practical accuracy and our own tests with simulated data.[53] The efficiency of an instrument and analysis method to determine lifetime changes is best described by the "*F* number":[54] the closer this is to unity, the more efficiently are available counts utilised in the lifetime determination. We regularly achieve an *F* number of 2.6, indicating that we can routinely obtain this 3% resolution with a reasonable 7000 photon counts per pixel. More recent developments, based on Bayesian approaches, suggest that *F* numbers below 1.5 are feasible (P. R. Barber and B. Vojnovic, personal communication), suggesting that the photon count per pixel can be decreased by at least a factor of two for the same level of accuracy. This can be compared to Elder et al.,[55] who used FD-FLIM techniques for the determination of FRET. Elder et al. found FD-FLIM signal-to-noise ratios to be 4–5, while we generally obtain a signal-to-noise ratio of 15. In contrast to intensity-based FRET measurements, FLIM-based FRET measurements can also filter out artefacts introduced by variations in the concentration and emission intensity across the sample.

### 2.2. Selection of Donor and Acceptor Molecules

Common to all FRET measurements is the appropriate selection of donor and acceptor molecules. A hint for the selection of such a FRET pair can be taken from the fluorophores' spectral information, that is, the excitation spectrum of the acceptor should overlap with the emission spectrum of the donor fluorophore, while the acceptor fluorophore should not be significantly excited at the excitation wavelength of the donor fluorophore. The latter is imperative for measurements relying on SE/APB, while donor lifetime measurements are not affected. Furthermore, resistance to photobleaching is another impor-

**Figure 2.** Principle of FRET and examples of successful experiments involving either genetically encoded fluorophores or labelled antibodies as FRET pairs. A) Schematic Jablonski representation of basic photophysical processes relevant for FRET. B) Top: absorption spectra of the orange/red fluorescent proteins mOrange, mRFP1, and mCherry overlapping with the absorption and the normalized emission spectra of GFP. Bottom: Calculated overlap integrals and Förster distances R (inset) for the FRET pairs GFP-mOrange, GFP-mRFP1, and GFP-TagRFP. Spectral data were retrieved from the Tsien laboratory website (http://www.tsienlab.ucsd.edu/). C) Detection of the direct protein–protein interaction between the receptor tyrosin kinases Her2 and Her3 in breast cancer cells. Both receptors were labelled with genetically encoded fluorophores (Her2 was fused to GFP and Her3 to mRFP1). There is a certain basal level of heterodimerization between these molecules as proven by a slightly reduced fluorescence lifetime when both fusion proteins are expressed in the same cell (compare top and middle rows). Importantly, upon stimulation with neuregulin-1 (NRG), the receptors heterodimerize. This is reflected by a higher FRET efficiency, that is, a warmer colour in the fluorescence lifetime map in the bottom row. D) Cumulative FRET efficiency histograms are shown for the images in the middle and bottom row of (C). E) Detection of intermolecular FRET between directly labelled anti-ezrin IgG-Cy2 and anti-phospho PKCα (T250) IgG-Cy3 in breast tissues, by two-photon FLIM. The images represent an example of invasive breast cancer, in which membranous ezrin:PKCα colocalisation is seen (white arrows) and which corresponds to the region of increased FRET Eff due to ezrin:PKCα interactions (black arrow). The anti-phospho PKCα (T250) IgG cross-reacts with an 180 kDa non-PKC protein that is located mainly in the nucleus, giving rise to the non-specific nuclear staining.[70] The non-specific staining does not however interfere with the determination of FRET by donor FLIM.[133,134] As a negative control, anti-phospho PAK-1 (T423) IgG was conjugated to Cy3 at the same ratio and applied to the adjacent TMA section. As expected, it was found not to interact with ezrin. F) Cumulative FRET efficiency histograms are shown for the images in (E).

  

tant fluorophore characteristic, especially in SE/APB experiments where separate images must be taken. For FLIM-based imaging, photobleaching is not much of an issue for the acceptor fluorophore; however, the donor fluorophore must not photobleach within the observation window. Furthermore, photobleaching of the donor will discriminate against the donor population that does not undergo FRET as these molecules are more likely to photobleach[56,57] [this principle has been employed in the so-called donor photobleaching fluorescence resonance energy transfer (pbFRET)]. Consequently, the photobleaching time of the donor fluorophore varies inversely with its fluorescence lifetime.

A good example of how the available techniques can affect the selection of a FRET pair is outlined in the following. Monomeric green fluorescent protein (mGFP) is a very bright and photostable genetically encoded fluorophore that exhibits a single exponential lifetime decay.[48] It is suitable for SE/APB as well as FLIM-based FRET measurements. However, selecting a suitable acceptor fluorophore to form a FRET pair is more delicate. Generally, the Förster radius and the overlap integral determine whether two fluorophores might form a suitable FRET pair, but this is not always sufficient. For instance, the mRFP1-derived mOrange, which has a larger overlap integral with mGFP than both mRFP1 and mCherry (Figure 2B), was found to perform very badly when compared to mRFP1 and mCherry in FRET experiments with identical amino acid chains linking mGFP to the mRFPs.[58] The reason for this unexpected behaviour of mOrange is not well understood yet, but may be due to relative orientation-dependent effects (calculation of the Förster radius assumes two independent fluorophores rather than linked fluorophores as used in these experiments). For the FRET pairs GFP-mRFP1 and GFP-mCherry we calculated the Förster radius to be 5.2 and 5.3 nm, respectively, which were in agreement with the literature.[48,59] When these FRET pairs were fused with identical linkers or within a biosensor construct it was shown that mRFP1 is a slightly better acceptor for mGFP than mCherry (higher FRET).[58] However, mRFP1 is less photostable than mCherry[60] and therefore, while being the RFP of choice for FRET-by-FLIM, problematic for ratiometric SE/APB experiments. As an example, we show the application of FRET imaging to study receptor oligomerisation involving the mGFP-mRFP1 FRET pair in human breast cancer cells (Figure 2C/D). The two receptor tyrosine kinases Her2 and Her3 were expressed as chimeras that were fused on their C-termini with either mGFP or mRFP1. Upon treatment with the Her3 ligand neuregulin-1, the oligomerisation state of the two receptors increases as determined by an increase of FRET. The Her2/Her3 heterodimer will be an important cancer target for screening small molecules or siRNA libraries using high content (HCM) or high throughput microscopy (HTM) since it has been purported to be a potent mitogenic and oncogenic unit for a variety of cancers.[61] Recently, an engineered variant of an Entacmaea spp.-derived red fluorescent protein, TagRFP, was reported, which was found to be a good acceptor for GFP in FRET-by-FLIM experiments (our unpublished results and [62]). The Förster radius of the GFP/TagRFP pair was determined to be 5.8 nm and is significantly longer than that for GFP/mRFP1 or GFP/mCherry pairs. If the FRET pairs are chosen carefully, it is possible to monitor different interactions at the same time in a live cell. As a proof of concept, this has been shown for two caspase sensors in the same cell.[63] Very recently, this concept was applied for the measurement of caspase-3 activity alongside calcium levels in apoptotic cells.[64] With the development of chromoproteins, which are barely fluorescent and can act as FRET acceptors,[65] and with further shifting the spectral properties of fluorescent proteins towards the near-infrared region,[66] it might soon become possible to monitor even more than two different co-existing FRET pairs in the same living cell.

If FRET is determined by donor FLIM measurements, the decay function of the donor lifetime is also an important factor. In classical FLIM analysis, the data are fitted to single-, double,- or multi-exponential decay functions in order to determine the fluorescence lifetimes from these curves. For sufficiently accurate fitting to a single-exponential decay more than 1000 photons are generally required.[67] In the absence of any acceptor, a donor fluorophore that exerts a single-exponential decay (e.g. GFP[48]) is favourable over a donor fluorophore exerting a multi-exponential decay (e.g. CFP[68]). This is because in the presence of FRET any exponential decay becomes of higher order. Thus, fluorophores with multi-exponential decays in the absence of FRET require at least an order of magnitude more photons and, consequently, it is more time-consuming to reach the same level of accuracy. Recently, phasor analysis was adapted for time-resolved FLIM providing an analysis technique that avoids the use of any a priori information such as the exponential decay model for data fitting.[69] But phasor analysis is not without its problems, not least is the need to determine the background photon count independently. Bayesian methods look promising for robust lifetime determination from low-photon-count data which may reduce acquisition times significantly.[53] In addition, this way of data analysis provides a significant benefit in the speed of analysis as compared to classical pixel-by-pixel fitting, which will be important for larger-scale FLIM-based screening efforts.

If there is no suitable expressible probe (Table 1) or the experimental setup does not allow for the use of genetically encoded fluorophores (e.g. a tagged protein can behave differently from its untagged counterpart, human tissue samples), organic dyes offer many more opportunities. Many organic dyes covering the whole of the UV/VIS and NIR spectra have been developed, and several have been used for FRET imaging experiments (Table 2). In principle, the same photophysical and equipment-related decisions as compared to expressible fluorophores need to be made when selecting any of those for a FRET experiment. Organic dye-labelling can be performed either 1) during chemical synthesis of the probe, 2) by coupling fluorophores to otherwise non-fluorescent probes for specific labelling (e.g. antibodies[17,18,70,71]), or 3) by specifically targeting a (leuco-)fluorophore to genetically tagged molecules of interest (e.g. FlAsH/ReAsH to tetracysteine motifs[72] or O6-benzylguanine/O6-benzylcytosin-labelled dyes to SNAP/CLIP-tagged proteins, respectively[73,74]).

  

**Table 1.** Genetically encoded fluorophores suitable for FRET pairs.

| Donor | Acceptor | References |
|---|---|---|
| mAmetrine | tdTomato | [63] |
| Sirius (UMFP-4) | mseCFP | [64] |
| mCerulean ~CyPet[a] > (m)ECFP | YPet > mCitrine ~mVenus[c] > EYFP | [27,32,33,135–142] |
| mTFP | YFP, mCitrine | [63,143] |
| mTurquoise | mVenus | [144] |
| TSapphire | mOrange,[b] dsRed | [64,145] |
| mUKG, MiCy | mKO[d] | [146,147] |
| (m)EGFP, AcGFP1, TagGFP | mRFP,[c] TagRFP, mCherry[d] | [48,62,148–150] |
| (m)EGFPΔCT | mRFP,[c] mCherry[d] | [58] |
| (m)GFP | REACh2[e] | [65,151] |
| mKO | mCherry | [152] |

[a] CyPet has a more blue-shifted and narrower emission peak as compared to Cerulean, but matures inferior at 37 °C; [b] mOrange is not recommended if photostability is critical or when it is targeted to compartments of low or changing pH;[60] [c] Recommended as acceptor only for FLIM as its photobleaching is significant; [d] Recommended for ratiometric measurements due to its good photostability; [e] REACh2 is a chromophore rather than a fluorophore.[65]

**Table 2.** FRET pairs used in imaging experiments including at least one organic dye.

| Donor | Acceptor | References |
|---|---|---|
| EDANS[a] | DABCYL[b] | [153] |
| 6-chloro-7-hydroxycoumarin | DiSBAC2(3)[c] | [154] |
| Dapoxyl sulfonamide | Alexa594, dsRed | [155,156] |
| ECFP | FlAsH[d] | [157,158] |
| Alexa350 | Alexa488,[h] Alexa594[h] | [159] |
| BG-K[e] | BG-d2,[f] Alexa647 | [73,160] |
| Fluorescein/FITC | Disperse Red 1 (quencher), TRITC, Alexa555 | [161–163] |
| Alexa488 | Alexa546, Alexa594 | [159,164,165] |
| FlAsH, EGFP | ReAsH[d] | [149,166] |
| EGFP | Cy3, Alexa546, Cy3.5 | [15,17–21,70,71,167] |
| BODIPY[g] | Rhodamine | [31] |
| Alexa546 | Cy5 | [168] |
| Cy3 | Cy5 | [70,169] |
| Alexa680 | QSY-21 (quencher) | [170] |

[a] EDANS is 5-((2-aminoethyl)amino)naphthalene-1-sulfonic acid, [b] DABCYL is 4-(dimethylaminoazo)benzene-4-carboxylic acid; [c] DiSBAC2(3) is bis-(1,3-diethylthiobarbituric acid)trimethine oxonol; [d] FlAsH and ReAsH stand for fluorescein arsenical helix binder and resorufin arsenical helix binder, respectively, and bind specifically to CCPGCC motifs; [e] BG-K is a cell impermeant far-red dye covalently linked to $O^6$-Benzylguanine for coupling to the SNAP-tag. The substrate specificity of the SNAP-tag is orthogonal to the one of the CLIP-tag, thus allowing for specific labelling of two different proteins in live cells. The combination of CLIP- and SNAP-tags is promising for future FRET studies; [f] BG-d2 is a cell impermeant UV-excitable europium cryptate pyridine-bipyridine (Eu–PBBP) dye with a large Stokes shift covalently linked to $O^6$-Benzylguanine for coupling to the SNAP-tag; [g] BODIPY is 4,4-difluoro-4-bora-3a,4a-diaza-s-indacene and belongs to the boron-dipyrromethene dyes; [h] Free Alexa488,[171] Alexa594,[172] and DyLight594[172] dyes were found to have single-exponential fluorescence lifetime decays. If Alexa594 or DyLight594 were attached to IgG they showed bi-exponential behaviour.[172]

The classical example for the detection of protein–protein interactions was the use of fluorescently labelled antibodies.[70,71] Unless more sophisticated site-specific labelling strategies are applied, labelling results in a population of antibodies with different dye-to-protein ratios. In addition, dye conjugation might interfere with antigen recognition. This is especially an issue if high dye-to-protein labelling ratios are necessary due to low abundance of antigens or low-affinity antibodies. For a successful antibody-based FRET experiment there are further considerations necessary regarding the dye-to-protein ratios and the Förster radius. Antibody pairs were found to perform best in FRET experiments if the antibody linked to the donor fluorophore was labelled at a dye-to-protein ratio of 1:1, while the antibody linked to the acceptor molecule was labelled at a ratio of 3:1.[75] As for the Förster radius, it is important to keep the donor and acceptor fluorophores within distances where FRET can occur. Consequently, the use of directly conjugated primary antibodies is always preferable over the use of a combination of primary and labelled secondary antibodies. The latter leads to increased distances of the fluorophores and diminishes a positive FRET signal and consequently the signal-to-noise ratio. If one of the fluorophores is a fluorescent protein, the use of a primary antibody in combination with a Fab-fragment of a secondary antibody was also shown to be successful (e.g. GFP together with Cy3- or Cy3.5-labelled Fab-fragments[18,70,71]). Antibody-based strategies are mostly applied to experiments involving fixed cells, because their delivery into a live cell is difficult as they are cell-impermeant. However, several other fluorescent probes and even some leuco-fluorophores (e.g. far-red O6-benzylguanine and -cytosin dyes) share this disadvantage with antibodies and need to be microinjected into cells if live experiments are desired. The latter is a significant shortcoming for the setup of any live cell screening assay or intravital experiment (see below). On the contrary, antibody or antibody-like molecule (e.g. DARPin[76])-based FRET experiments are one of the few pragmatic options for the direct visualization of protein-protein interactions in human tissue. Fluorophore-conjugated antibodies can be used on either frozen or formalin-fixed paraffin-embedded tissues collected from patients. As an example for an antibody-based FRET assay, we show the direct interaction between the cytoskeletal protein ezrin with phosphorylated protein kinase C alpha in tissues derived from breast cancer patients. This is a phenomenon that was first reported in breast cancer cells,[18] but was found not to be cancer type-specific.[18,77] While a larger tissue study is currently in progress in our laboratory, Figure 2E,F shows a typical result proving the interaction of these two proteins and thereby suggesting that PKC$\alpha$ is involved in the phosphorylation of ezrin in breast cancer tissues and that this phosphorylation (at Thr-567) may be implicated in the metastatic relapse of these patients.[78–80]

  

## 3. FRET Screening: State-of-the-Art Imaging Techniques and their Throughput

Although microscopy has always been a favourite tool in cell biology, for long time it suffered from being solely descriptive and the unbiased discovery of novel pathways or interactions between them has been difficult. With the establishment of automated high-content (HCM) and high-throughput microscopy (HTM) in combination with RNAi-based knock-down techniques this limitation could now be overcome.

The first groundbreaking HTM work was a recent phenotypic profiling study by the MitoCheck consortium (www.mitocheck.org) screening 21 000 protein-coding human genes using fully-automated time-lapse wide-field epi-fluorescence HTM[81,82] for imaging fluorescently labelled chromosomes in live human cancer cells (HeLa) stably expressing histone H2B fused to GFP. Collecting and analysing data of more than 19 million cell divisions, this screen identified 1249 genes involved in mitosis (5.95%). Further validation by additional independent RNAis and complementation assays confirmed 572 mitotic hits (2.72%).[8] A systematic analysis of about 700 proteins, most of them overlapping with these mitotic hits, aimed at the identification of their precise cellular localization and protein binding partners.[7] The authors used bacterial artificial chromosomes to express tagged proteins, purified them via a biochemical tandem-affinity approach and identified binding partners via tandem mass spectrometry. This strategy resulted in 239 purified proteins (34.3%) and the identification of 936 binding partners corresponding to 2011 specific pair-wise protein-protein interactions (www.ebi.ac.uk/intact, identifier IM-11719). However, significant information on potential protein-protein interactions proved not to be accessible due to the low rate of purified proteins (34.3%). Furthermore, protein–protein interaction dynamics can only be studied crudely with this biochemical technique. Large-scale HTM screening approaches clearly will be very useful in the future to also investigate other cellular processes like cell migration and adhesion, cytoskeletal dynamics, endo- and exocytosis as well as protein secretion, protein trafficking and degradation, nuclear functions, programmed cell death, or the consequences of viral infections. However, while such phenotypic HTM screens are invaluable for the identification of novel components of a cellular process, they can be complemented by a variant of HCM/HTM based on direct protein-protein interaction imaging,[10] in order to provide additional insights.

In phenotypic screens, there is also the issue of quantification as they rely on scoring systems and sophisticated pattern recognition software. Although, the algorithms can be ultimately trained to be objective, the classification of the phenotype and/or its boundaries introduce an element of subjectivity. The cell morphology often represents a readout that is the integrated outcome of several signalling subnetworks and deconvolution into specific pathways is usually very complex. The assessment of individual protein-protein interactions specific to a particular pathway or sitting at the junction of several pathways could allow for a clearer readout. Furthermore, many phenotypic HTM screens rely on widefield microscopy which does not offer sufficient spatial resolution to distinguish between different individual protein complexes.

In contrast, FRET imaging, though relying on far-field optical arrangements, is a near-field technique which offers access to quantitative information on complex formation and dissociation on a molecular level. Recent developments improving automated high resolution FRET imaging enabled the direct spatiotemporal accessibility of protein-protein interactions of live cells. Due to the extremely high specificity of a studied protein–protein interaction in FRET experiments the number of false positives is also expected to be significantly lower in such screens (c.f. 54.2% in the abovementioned phenotypic HTM screen[8]).

Figure 3 shows an example of a TCSPC-based FRET-by-FLIM screen for small-molecule compounds interfering with the specific interaction of two signalling molecules linking a mitogenic with an apoptotic pathway in cancer cells. Mammalian sterile 20-like kinase-2 (Mst2) is an inducer of apoptosis upon stress and tumour suppressor signals. Its pro-apoptotic kinase function is abrogated by complex formation with RAF proto-oncogene serine/threonine-protein kinase (Raf1, c-Raf),[83–85] This is a result of an upregulated Akt kinase pathway[86] leading to dysregulation of this Mst2-dependent pro-apoptotic pathway and eventually can result in unlicensed growth in cancer cells. In Figure 3 we show results of a typical FRET-by-FLIM HCM screen for small molecule modulators of the Mst2-Raf1 interaction. The assay is based on a novel biosensor consisting of Mst2 and Raf1 domains and a FRET pair (mGFP and mRFP1) reporting on the interaction. Two hits from this screen are shown as examples; "compound 27" was found to disrupt the specific interaction of Mst2 with Raf1 and therefore exerts the desired pro-apoptotic effect in cancer cells while a different compound, "compound 73", was found to promote this interaction. Conventional FRET-by-FLIM screens are still somewhat slow with photon counting rates rarely exceeding $10^6$ $s^{-1}$, but they are very precise. However, improved data analysis methods (fitting algorithms, global analysis[43]) have the potential to reduce the imaging time significantly by making more efficient use of available counts.

## 4. Integrating High-Content Imaging Data into Knowledge about Cancer Proteome Sensitivity

High-throughput and high-content imaging data can be fed into the framework of publicly available gene and protein interaction networks, which can be used for instance to analyse cancer proteome sensitivity (by comparing the effects of knockdown of individual genes on their 'neighbours' according to their relative degree of separation on the network). Rather than being a static resource, networks can be expanded or updated as the results of new experiments arise, generating a loop that cycles between predictions and experiments leading to more sophisticated and refined models.

  

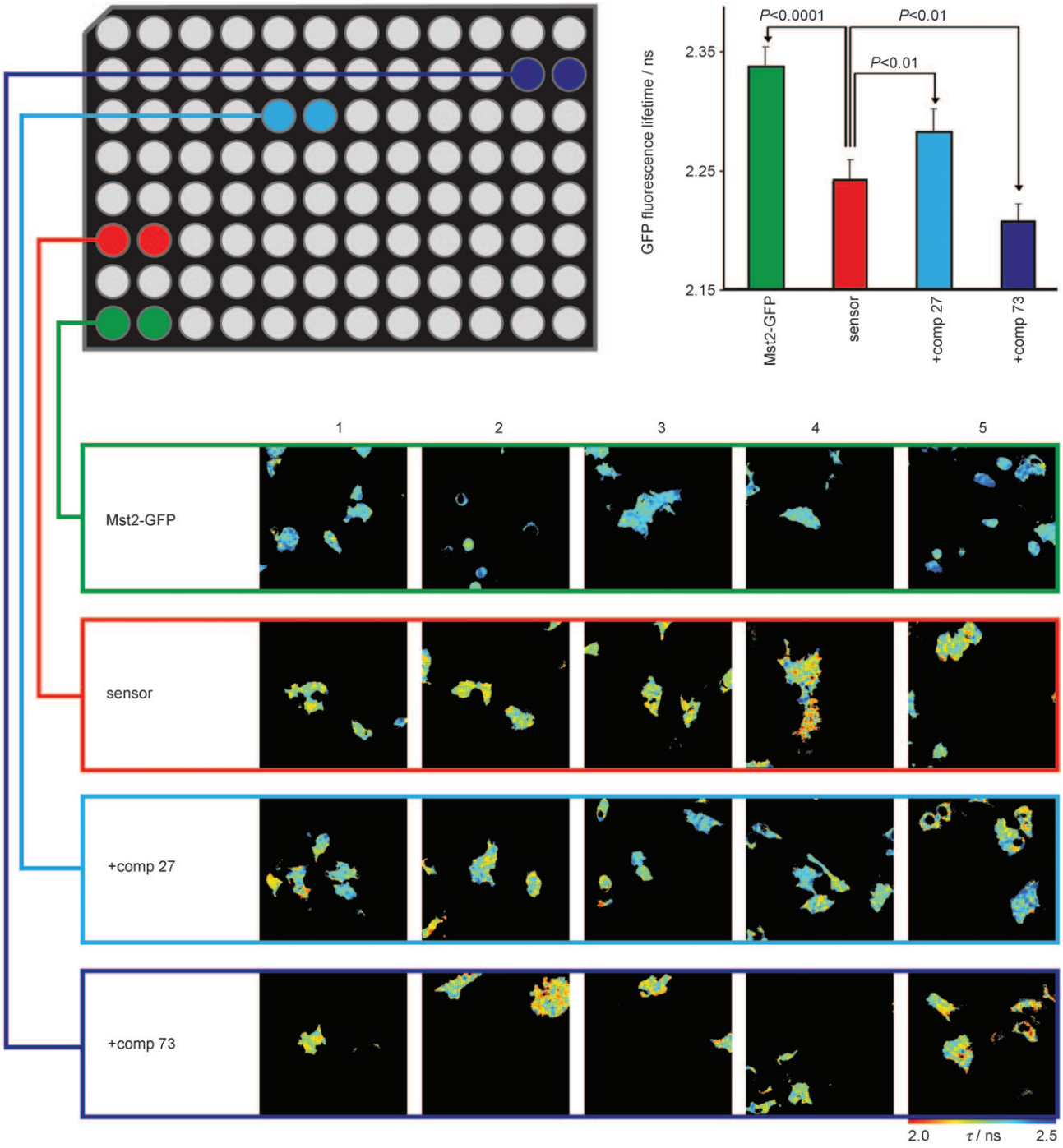


**Figure 3.** Drug screening assay for modulators of the specific interaction of Mst2 and Raf1 in breast cancer cells. Cells expressing a biosensor reporting on the direct protein–protein interaction between Mst2 and Raf1 were treated with different small molecule drugs. All drugs were tested in duplicate and ten different regions over the two microplate wells were imaged using a purpose-built automated single-photon FLIM setup. Five of the ten different regions are shown to illustrate the consistency of the FLIM measurements over various regions in the two wells. (Red) Cells expressing the biosensor in the absence of drug treatment. (Cyan) Cells expressing the biosensor that were treated with drug number 27; the latter was found to interfere with the interaction between Mst2 and Raf1. (Dark blue) Cells expressing the biosensor that were treated with the drug number 73, which was found to positively affect this interaction. (Green) Cells expressing Mst2-GFP were used as an internal control for the determination of the absolute lifetime values and the function oft he biosensor. The top right panel shows the average fluorescence lifetimes plus standard deviation of the cumulated results of all images taken in this assay.

### 4.1. Building a Protein Interaction Network Using Computational Biology

Protein interaction networks (Figure 4) portray a global picture of the extracted interacting partners, but the direct relation of individual protein interactions to specific cellular functions and dynamics remains still challenging to extrapolate. On the other hand, the detailed analysis of a particular cellular function or pathway that may be analysed and extracted in the context of

  

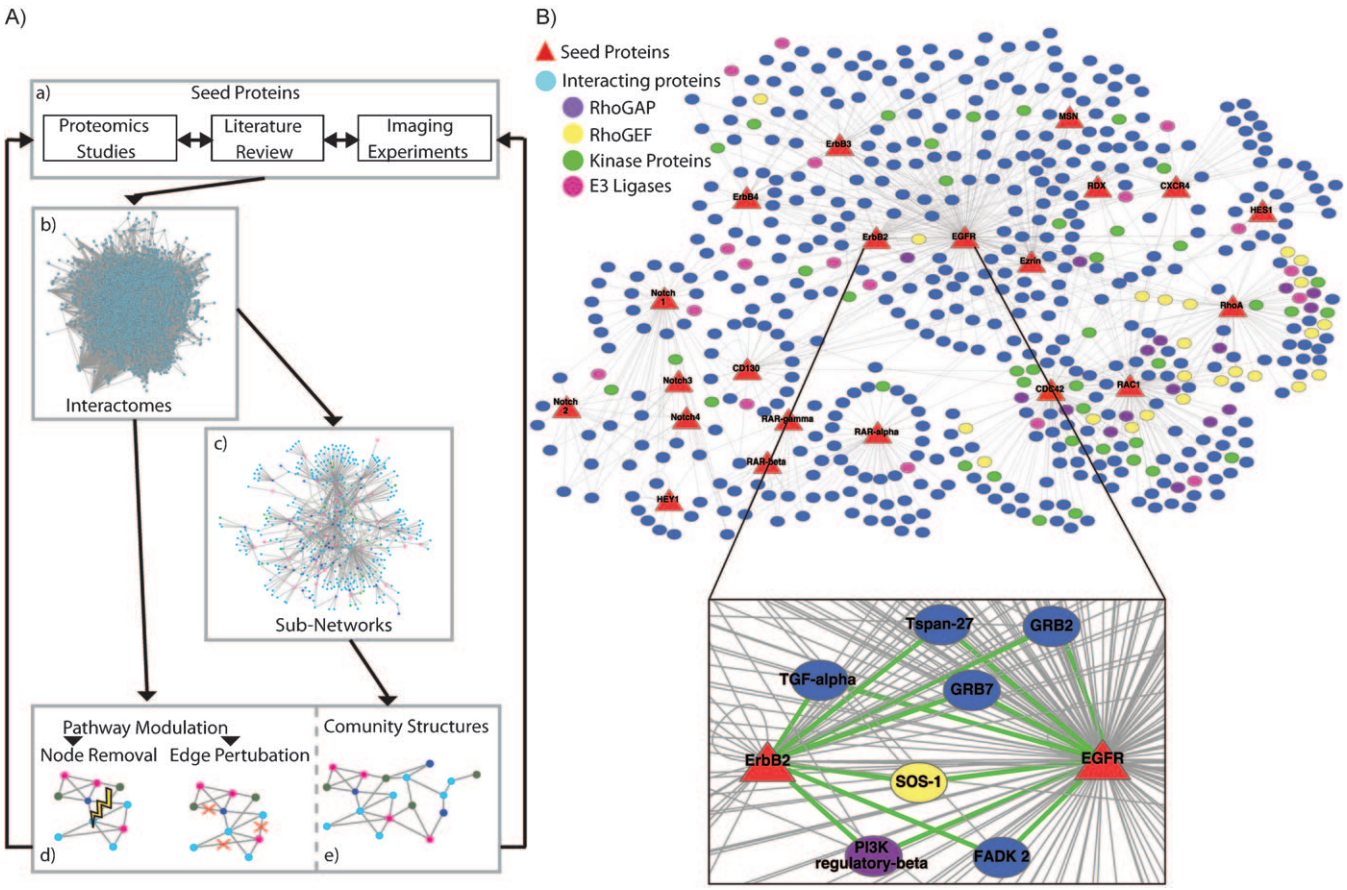


**Figure 4.** Scheme for the generation of a protein interaction network including an example. A) Schematic representation of the procedure followed for the functional analysis of phenotype associated subnetworks. a) High-throughput experimental data derived from a variety of experiments (proteins chips, microarrays, ChIP-Seq, RNA-Seq) currently available from public databases can be integrated with both information previously described in literature and with data newly generated by in-house experiments. This procedure can be used to identify sets of "seed proteins" specific to the biological processes/pathways under investigation. b) Large-scale maps of protein-protein interactions (interactomes) can be mined for interactions that involve the previously indentified "seed proteins". The selection criteria following the principle of "guilt by association" can be applied to immediate partners or partners of partners. c) The extracted proteins and interactions constitute subnetworks that can be integrated with available biological data. Following this procedure the subnetworks embed specific knowledge associated to the studied system and they can be used to propose new experiments. d) Information can be extracted by interfering with a particular system or pathway embedded in the network. This could be achieved by either completely removing one node (left panel) or by disrupting specific interactions without affecting other parts of the network (right panel) e) A series of algorithms can be used to identify network regions that are enriched for proteins of a given function or modules with a higher then average interconnectivity, These regions are commonly referred to as "community structures". B) Metastatic phenotype subnetwork for two receptor tyrosine kinases, EGFR/ErbB1/Her1 and ErbB2/Her2 ("seed proteins", red triangles). A subset of that subnetwork is shown in the inset, and visualizes how the two seed proteins are interconnected via different protein interaction partners. The proteins in the subnetwork are colour-coded according to their domain architecture as shown in the legend with interaction partners represented by ellipses. The whole fully annotated subnet is available in the Supporting Information.

specific diseases may benefit from the study of smaller, accurately selected sub networks.[12] In order for such an approach to be feasible, the selection of relevant subnetworks must be accurate and reliable, extracting the interactions that play a determinant role in the studied process. Therefore, a fine balance must be used in selecting from a global network only a small number of relevant interactions to focus on, without excluding crucial proteins. Essential to this selection process is the identification of a set of proteins termed "seed proteins". These proteins can be selected by using an educated guess of the "guilt by association" principles relating a small number of proteins that should be at the basis of a common mechanism causing the observed phenotype (e.g. the "metastatic" phenotype). Candidate proteins are typically selected based on prior knowledge of the system under investigation, making use of information from literature, from specific experiments or from merged data. Once seed proteins are identified, all the interactions involving such proteins are extracted along with interactions between their direct partners, giving origin to a subnetwork. Direct partners of the selected proteins tend to provide a more accurate functional association but in some cases partners of partners can also be considered. Studied systems or pathways can vary tremendously in nature and implications for cellular function, therefore the criteria used to select seed proteins must also reflect the properties of the system and the aims of the study. For example, if the aim of a given study is to understand the mechanism of a particular disease, then a set of seed proteins can be chosen on the basis of proteins

  

previously known to be associated (genetically or from any other source) with that disease. Transcriptional profiling has become a standard technique in the last decade and a large number of diseases have now been characterized by this approach, therefore this experimental source can be very useful for the identification of important subnetworks.[87,88] Genes found to be differentially expressed in disease tissues can be used as seed proteins and subnetworks can be constructed around those proteins and their interactions. Platzer et al. used information derived from transcriptional profiling of a series of tumours to construct tumour specific subnetworks, which were later analysed using a series of network theory-based measures.[89] They concluded that several tumours have functional dependencies on particular proteins and those proteins can be identified on the basis of transcriptional profiling. Furthermore they proposed that a robustness analysis of tumour subnetworks might yield novel therapies with higher specificity and smaller chance of developing resistance.

An example of a seed protein (ezrin) that is associated with a membrane receptor-cytoskeletal linkage function, causing the "metastatic" phenotype, is shown in Figure 2E. The application of FRET imaging in live and fixed cells has significantly improved our understanding of the molecular pathways by which extracellular and environmental signals are sensed by these membrane receptors, transduced through the cell signalling machinery, in order to trigger remodelling of the cytoskeleton, thus leading to cancer cell invasion and metastases. We have now attempted to connect in a human proteome subnetwork (Figure 4B) that includes many of the cell adhesion/trafficking/motility-related "seed proteins" (red triangles), and the relevant protein-protein interactions thereof;[15,17,18,20,21,70,75,90–95] as well as the post-translational modifications and associated conformational changes,[28,39,40,65,70,96–103] which have been imaged in cancer cells and tissues.

### 4.2. Construction of Functional Modules within Protein Interaction Networks

Each protein in the network is annotated as a node and its interactions with other proteins as either binary or weighted undirected edges. Once the relevant subnetworks are created and the confidence of the reported interactions has been reinspected, the question remains on how to extract the most relevant interactions and proteins in the specific subnetwork. This problem is normally referred to as node or interaction prioritization since it requires the identification of a set of rules or properties in order to recognize the most influential nodes or interactions. A series of methods have emerged to take advantage of classical topological properties of networks such as the degree distribution, clustering coefficient, vertex betweenness and shortest path measures in order to identify key nodes. Typically these methods rank nodes according to a specific topological property. Highly ranked nodes are assumed to represent proteins that are responsible for the dissemination of signals and information flow across the networks. Lee et al.[104] developed a subnetwork specificity score, which ranks the specificity of each node to its subnetwork. They proposed that the higher the rank, the more relevant the protein is to its subnetwork. In some circumstances it is not only important to identify the most significant nodes or interactions in a subnetwork but also all the relevant units that might constitute a "functional module". Functional modules might in some cases be represented by a series of proteins and interactions that constitute a pathway or a single molecular complex with a predefined function. Many functional modules tend to have a high density of connections between its members when compared with connections to proteins outside the module. This property is termed "community structure" and it has been extensively used along with other network properties to detect functional modules.[105–107] Another approach to prioritize nodes or interactions is to develop a more ad-hoc solution that can integrate aspects specific to the system under investigation. For example, this can consist of selecting only those proteins that are composed of a particular domain of interest or any other suitable characteristics. For high-content screens, rather than targeting the entire genome by using RNA interference (RNAi) or by blocking protein activity/function with specific inhibitors, specific perturbations can be applied to gene components of these modules, which represent smaller and accurately selected subnetworks for systems perturbation.[12]

### 4.3. Generation of a Weighted Protein Interaction Network

The conformation/activity of the nodes (seed proteins) and thereby their ability to form the associated edges can be quantified by the FRET efficiency (Eff) values obtained in cells expressing various fluorescent sensors (refs. [9,16,39–43] and Figure 3). The effects of individual RNAis against different gene/protein components, on these chosen nodes and edges, can then be weighted using the Eff values obtained. The relationship between the concentrations of both free and complexed forms of the seed proteins that are monitored and the Eff values obtained from such experiments is described in our recently published example.[40]

From these high-content imaging screens one can calculate system response profiles (SRPs) of the cells, which represent probabilistic estimates of the changes in the conformation/activity of each of, for instance, 21 monitored protein molecules (seed proteins in Figure 4B) within the network/module/subnetwork, following each of the 550 expression perturbations. These data, in the form of a table of $21 \times 550 = 11\,550$ histograms can be used in two ways. First, they can be used to measure retrospectively (and improve) to what extent the chosen subnetwork captures the dominant pathways in which the seed protein participates. For instance, comparing the observed number of functional interactions in the SRP (responses with a statistically significant deviation from zero) to what would have been predicted for random samples of 550 proteins from the human proteome tells us to what extent the subnetwork can be regarded as a distinct module. Second, the columns in the final SRP table (representing the response characteristics for each expression perturbation) can be used as 550 input vectors (each of dimension 21) to a self-organising map (SOM).[108] A SOM is an artificial neural network, trained

  

using unsupervised learning, to produce a two dimensional representation of high-dimensional data. This network, in this biological context, can be employed to detect and represent the mutual relations between the various subnetwork regulators. SOMs have been previously employed to present temporal changes in the normalised expression pattern of constituent genes within a small number of gene subnetworks/clusters during for example, cell cycle progression.[109] Here, upon application to the SRP columns and upon colour-coding the 550 relevant genes according to their column norms (giving the overall impact of their perturbation) one obtains a clear and practical two-dimensional representation of the key regulators of the subnetwork, which reports their overall relevance and their mutual relations. We are now in the position to execute the above protocol for integrating objectively our biological, bioinformatical, and experimental evidence, in order to identify the key players in the human protein subnetwork that are responsible for controlling cancer cell adhesion/motility/invasion.

## 5. FRET Imaging in Preclinical Tumour Models

Once individual genes and small molecules are identified through high content/throughput imaging, they can be validated in preclinical in vivo models using the same fluorescent sensors and probes. There are many aspects of the tumour micro-environment which cannot be adequately modelled in vitro. These include the presence of a wide range of normal cells which can influence the motility of tumour cells, the effect of blood flow and low levels of oxygen often found in regions of tumours some distance away form functional vessels. To discover the effect of these variables on the movement of tumour cells, in vivo models are required. There are several important objectives of preclinical imaging related to cancer research; 1) longitudinal tracking of the response of both primary tumours and secondary metastases during potential therapies including the assessment of potential tumour recurrence upon discontinuation of treatment; 2) monitoring the effects of drugs on complex biological processes such as changes in the vascular volume fraction in tumours, vascular leakiness, etc in response to treatments like the blocking of pro-angiogenic signals; 3) analysis of the pharmacokinetics and pharmacodynamics of potential drugs including dose optimization; 4) determination of the efficacy of a drug against the activity of its intended target. With the increasing importance of new biological entities targeting plasma membrane receptors that upon stimulation propagate signals intracellularly, the last of the objectives listed is a rather challenging one. FRET imaging of suitable biosensor molecules or specific protein–protein interactions is a very promising technology for dealing with this challenge. Importantly, existing FRET imaging techniques need to be adapted to enable intravital imaging of protein–protein interactions.

One way of preclinical intravital imaging of small laboratory animals is afforded be the means of whole-body imaging techniques. Using a well-designed apparatus, the spatial resolution can be comparable to low-power microscopic techniques on the surface of the tissue, but degrades considerably with depth. Below subdermal regions and towards the mid-body of for example, a mouse, the spatial resolution will be as poor as a few millimeters. Fluorescence lifetime measurements in such whole-body imaging devices have been reported.[110–112] Alternatively, trans-illumination can be used to counteract this phenomenon. The latter is the case in fluorescence lifetime tomographic techniques. The combination of FLIM with optical projection tomography (OPT[113]), so-called FLIM-OPT,[114] can improve the resolution of this technique from the mm-range to about 100 μm, but at the expense of imaging depth and imaging time. Recently, measurements using FRET-based probes were reported.[115] An alternative way of improving spatial resolution is accepting only early arriving photons and rejecting late-arriving highly scattered photons (early photon tomography[116]). Inevitably this increases the image collection time significantly.

It would be desirable to assess the efficacy of a drug on its intended target while monitoring a downstream signalling pathway, because for the latter the discrimination of crude cellular structures such as plasma membrane, cytosol and/or the nucleus will be required. Therefore, intravital imaging techniques offering microscopic resolution are desirable. Intensity-based intravital imaging techniques (including the use of window chamber adaptations), that involve cell tracking and determination of the subcellular localisation of proteins, has provided important cell biological information in the areas of morphogenesis, regeneration, and cancer.[117–124] For the reliable detection of protein-protein interactions in live animals, we have recently developed the use of deep-tissue fluorescence lifetime imaging (DT-FLIM). It requires multiphoton excitation to enable deeper penetration of the tissue[125] combined with laser scanning and offers z-sectioning capability. Recently, we have successfully adapted a bespoke two-photon system for DT-FLIM measurements, and we could show for the first time the reliable and repeatable determination of fluorescence lifetimes in a live mouse.[91] Figure 5 A shows an example of imaging data obtained in a live mouse carrying a xenografted tumour established from adenocarcinoma cells expressing a G protein-coupled receptor fused to mGFP. DT-FLIM measurements can be obtained from considerably deeper within the tissue than conventional microscopy would allow. In the example in Figure 5 A we also show that the measured fluorescence lifetimes barely change with increasing imaging depth, which currently allows their reliable determination in depth of up to 150 μm within the tumour. With increasing imaging depth there are also issues associated due to specimen-induced aberrations. This results in deterioration in both the image quality and resolution and is therefore restricting the depth at which one can image.[126] Adaptive optics, a technique originally developed for use in astronomy,[127] has been shown to be successful in overcoming problems associated with imaging in depth in confocal, multiphoton, CARS, and microscopy techniques using second and third harmonic generation.[128–132] The principle relies on altering the wavefront of the excitation beam with a wavefront modulator to compensate for the distortions introduced by the biological tissue sample. The success of such a technique relies on being able to correctly de-

  

termine the wavefront correction required. In microscopy, the wavefront is normally determined indirectly.

As optical imaging by microscopy is restricted to a penetration depth of less than one millimeter,[125] deeper tumours and distant metastasis, for example, in lymph nodes or the lung are generally not easily accessible for imaging. To circumvent this limitation, we have developed a fibre bundle-based fluorescence lifetime endoscope (FLE).[90] This new FLE technology permits studying tumours deeper than at the surface while still offering an optical resolution (~5 μm) sufficient to resolve individual cells (~15 μm for cancer cells in a 3D environment). Until now this technology has been used for measurement of FRET in cancer cells embedded in tumour-derived matrix gels as a phantom (Figure 5B). The measured FRET efficiencies in this model system have been in very good agreement with values obtained from cells in 2D culture grown on cover glass.[90] We expect this new technology soon to be used for intravital imaging applications in small laboratory animals.

While a compromise between optical resolution, imaging depth, field of view and imaging speed will always have to be reached, both concepts will prove useful complementary tools for preclinical imaging of protein-protein interactions in vivo. In the future the application of intravital FRET imaging will contribute significantly to the understanding of protein function as well as to the discovery and validation of drugs in preclinical models of cancer. In this respect FRET determinations by FLIM will generally have the advantage in being able to reject kinetic contributions from unwanted fluorophores. Nevertheless, long imaging times will be necessary in such cases and the use of NIR probes should always be seen as advantageous, provided their quantum efficiency is not restricting.

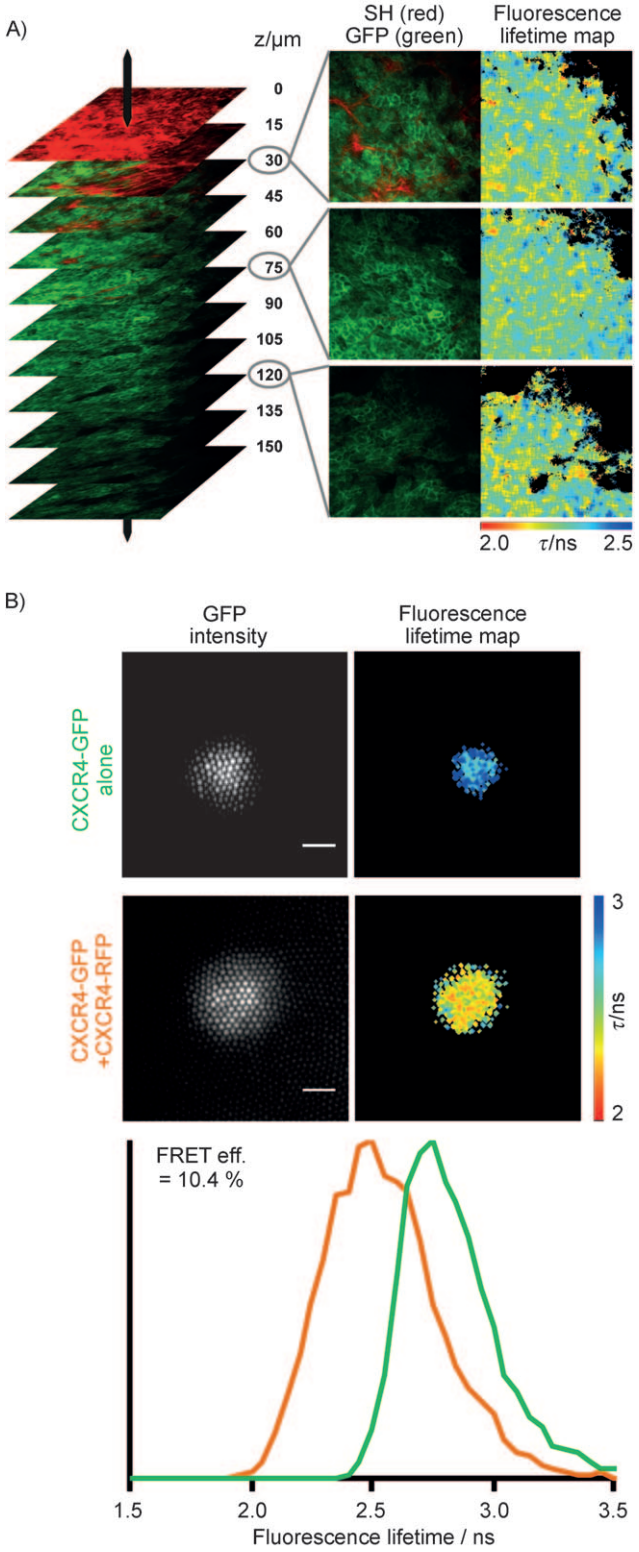


## 6. Outlook: Towards Systems Pathology[173]

The challenge of post-genomic medicine is to derive biomarkers that can predict clinical outcome to molecule-targeted therapies,[42] by unravelling the complex molecular networks within the proteome that drive biological function. In this context, the predictive performance of prognostic gene expression

**Figure 5.** DT-FLIM and FLE allow for the reliable determination of fluorescence lifetimes on a microscopic scale in vivo. A) DT-FLIM was used to acquire two-channel multiphoton fluorescence intensity images in a vertical stack beginning at the outer boundary of a xenoraft breast cancer tumour in a living mouse. Left: The fluorescence images of the two channels were pseudo-coloured; red: collagen fibres detected due to their second harmonic signal, green: GFP fluorescence of adenocarcinoma cells expressing a G protein-coupled receptor fused to GFP in their plasma membranes. Both channels were merged and aligned to the optical axis with numbers indicating the relative depth of the image plane as the distance from the outer tumour boundary. Right: Three planes of z-stack were selected as examples of the vertical stack and fluorescence lifetime maps were calculated from the time-resolved multiphoton GFP images. The fluorescence lifetimes in the images show similar distributions irrespective of the depth they were taken at, underlining that DT-FLIM is a robust technique, which gives reliable fluorescence lifetimes. The individual size of each image is 313×313 μm. B) Fluorescence lifetime endoscopy (FLE) of live cells embedded in a 3D matrix (Matrigel). Top: Time-resolved fluorescence images (scale bars 10 μm) were taken down a 2 m long fibre bundle with its end inserted in the 3D matrix. Cancer cells expressing the chemokine receptor CXCR4 fused to GFP or CXCR4 fused to GFP and mRFP1, respectively, were discriminated based on the differences of their fluorescence lifetimes. Bottom: Cumulated histograms of at least 6 different cells show a consistent difference in their fluorescence lifetimes. The calculated FRET efficiency was 10.4% and corresponds very well to the value obtained via conventional FLIM for cells in a 2D environment (10.9%, data not shown).

  

signatures has been found to be improved by incorporating protein interaction data.[174] Advances in imaging techniques have enabled tissue sample-specific detection of protein interactions and the post-translational modifications[70] that are necessary for these interactions to occur. Observing these interactions in patient-derived tissue samples could lead to significant refinement of prognostic models and better predictions of responses to anti-cancer drugs.

In order to understand how specific alterations in the protein interaction network relate to drug resistance or prognosis, it is first necessary to design a panel of protein interactions to be monitored in patient-derived tissue samples. System response profiles (SRPs, described in Section 4) derived from RNAi screens will inform on robustness and potential chemoresistance in the cancer proteome.[1] Network sensitivity analysis of SRPs can be used to detect fragile nodes within the cancer proteome and will identify candidate protein-protein interactions to be monitored in patient-derived tissue samples.

Given a panel of high-content imaging screens measuring protein interactions in patient-derived pathological tissue, the aim is to use this protein-level dataset to improve existing prognostic and treatment-response models. Discovery of clinically relevant image parameters of patient-derived tissue samples can be performed, for instance by clustering methods, using unsupervised multivariate analysis techniques including self-organising maps (SOM) and latent variable models.[175] An example was described above using a SOM for the analysis of multidimensional datasets acquired from cultured cells (Section 4.3). Predictive models of clinical outcome and response to drug treatment can be built using similar multivariate supervised techniques, whereby individual cancer tissue samples from presenting patients may be classified according to predicted outcome or treatment response.

Functional imaging of metastasis-associated protein interactions, such as the one depicted in Figure 2E, within cancer tissues will in the future offer clinically relevant information on patient-specific alterations in the cancer protein network. The monitoring of protein–protein interactions and prerequisite post-translational modifications will lead to an additional level of understanding of the differences between patient-derived cancer tissue samples and the relationship to clinical outcome and drug treatment response. High-content imaging applied to these patient samples can be used in combination with established clinically relevant assays that measure gene expression, single-nucleotide polymorphisms and DNA amplification and deletion events; as well as clinical and histopathological parameters. The addition of protein-level information is likely to improve predictive models of response to drug therapy for the individual patient, with an eventual aim of a personalised prediction of treatment outcome.

## Acknowledgements

*This work was supported by the KCL-UCL Comprehensive Cancer Imaging Centre, funded by Cancer Research-UK and the Engineering and Physical Sciences Research Council (EPSRC), in association with the Medical Research Council (MRC) and the Department of Health (DoH/England) [G.O.F., K.L., S.P.P.], a BBSRC grant [L.P.F., BB/H018409/1, and A.C.C.], an EC grant [G.W., LSH-CT-2006-037731], a Comprehensive Biomedical Research Centre award to Guy's & St Thomas' NHS Foundation Trust, in partnership with King's College London and King's College Hospital NHS Foundation Trust and a Cancer Research UK Clinical Training Fellowship [.G.P. 2008-09 and 2009-12, respectively], a Guy's and St Thomas' Charity grant [M.K., R041004], a Cancer Research UK Programme grant [P.R.B. and B.V., C133A/1812], an endowment fund from Dimbleby Cancer Care to King's College London [A.B., S.A.B., and T.N.], and grants from the MRC and the Leverhulme Trust [1U.1175.03.001.00001.01 and F/07040/AL to F.F.]. The FLIM systems were built with support from the MRC Co-Operative Group (grant G0100152 ID 56891), the UK Research Council (Basic Technology Research Programme grant GR/R87901/01), and the KCL-UCL Comprehensive Cancer Imaging Centre, funded by CR-UK & EPSRC, in association with the MRC and DoH.*

**Keywords:** bioinformatics · cancer · fluorescence · FRET · protein–protein interactions

[1] A. M. Xu, P. H. Huang, *Cancer Res.* **2010**, *70*, 3857 – 3860.
[2] R. Weissleder, M. J. Pittet, *Nature* **2008**, *452*, 580 – 589.
[3] P. R. Srinivas, M. Verma, Y. Zhao, S. Srivastava, *Clin. Chem.* **2002**, *48*, 1160 – 1169.
[4] L. P. Fernandes, A. Annibale, J. Kleinjung, A. C. C. Coolen, F. Fraternali, *PLoS One* **2010**, *5*, e12083.
[5] G. Gadea, V. Sanz-Moreno, A. Self, A. Godi, C. J. Marshall, *Curr. Biol.* **2008**, *18*, 1456 – 1465.
[6] V. Sanz-Moreno, G. Gadea, J. Ahn, H. Paterson, P. Marra, S. Pinner, E. Sahai, C. J. Marshall, *Cell* **2008**, *135*, 510 – 523.
[7] J. R. A. Hutchins, Y. Toyoda, B. Hegemann, I. Poser, J.-K. Heriche, M. M. Sykora, M. Augsburg, O. Hudecz, B. A. Buschhorn, J. Bulkescher, C. Conrad, D. Comartin, A. Schleiffer, M. Sarov, A. Pozniakovsky, M. M. Slabicki, S. Schloissnig, I. Steinmacher, M. Leuschner, A. Ssykor, S. Lawo, L. Pelletier, H. Stark, K. Nasmyth, J. Ellenberg, R. Durbin, F. Buchholz, K. Mechtler, A. A. Hyman, J.-M. Peters, *Science* **2010**, *328*, 593 – 599.
[8] B. Neumann, T. Walter, J.-K. Hériché, J. Bulkescher, H. Erfle, C. Conrad, P. Rogers, I. Poser, M. Held, U. Liebel, C. Cetin, F. Sieckmann, G. Pau, R. Kabbe, A. Wünsche, V. Satagopam, M. H. A. Schmitz, C. Chapuis, D. W. Gerlich, R. Schneider, R. Eils, W. Huber, J.-M. Peters, A. A. Hyman, R. Durbin, R. Pepperkok, J. Ellenberg, *Nature* **2010**, *464*, 721 – 727.
[9] D. R. Matthews, L. M. Carlin, E. Ofo, P. R. Barber, B. Vojnovic, M. Irving, T. Ng, S. M. Ameer-Beg, *J. Microsc.* **2010**, *237*, 51 – 62.
[10] H. E. Grecco, P. Roda-Navarro, A. Girod, J. Hou, T. Frahm, D. C. Truxius, R. Pepperkok, A. Squire, P. I. Bastiaens, *Nat. Methods* **2010**, *7*, 467 – 472.
[11] A. Esposito, C. P. Dohm, M. Bahr, F. S. Wouters, *Mol. Cell. Proteomics* **2007**, *6*, 1446 – 1454.
[12] R. A. Pache, A. Zanzoni, J. Naval, J. M. Mas, P. Aloy, *FEBS Lett.* **2008**, *582*, 1259 – 1265.
[13] D. J. Klinke II, *Cancer Res.* **2010**, *70*, 1773 – 1782.
[14] M. Caudron, G. Bunt, P. Bastiaens, E. Karsenti, *Science* **2005**, *309*, 1373 – 1376.
[15] N. Anilkumar, M. Parsons, R. Monk, T. Ng, J. C. Adams, *EMBO J.* **2003**, *22*, 5390 – 5402.
[16] S. J. Heasman, L. M. Carlin, S. Cox, T. Ng, A. J. Ridley, *J. Cell Biol.* **2010**, *190*, 553 – 563.
[17] J. W. Legg, C. A. Lewis, M. Parsons, T. Ng, C. M. Isacke, *Nat. Cell Biol.* **2002**, *4*, 399 – 407.
[18] T. Ng, M. Parsons, W. E. Hughes, J. Monypenny, D. Zicha, A. Gautreau, M. Arpin, S. Gschmeissner, P. J. Verveer, P. I. Bastiaens, P. J. Parker, *EMBO J.* **2001**, *20*, 2723 – 2741.

  

[19] M. Parsons, M. D. Keppler, A. Kline, A. Messent, M. J. Humphries, R. Gilchrist, I. R. Hart, C. Quittau-Prevostel, W. E. Hughes, P. J. Parker, T. Ng, *Mol. Cell. Biol.* **2002**, *22*, 5897 – 5911.
[20] M. Parsons, J. Monypenny, S. M. Ameer-Beg, T. H. Millard, L. M. Machesky, M. Peter, M. D. Keppler, G. Schiavo, R. Watson, J. Chernoff, D. Zicha, B. Vojnovic, T. Ng, *Mol. Cell. Biol.* **2005**, *25*, 1680 – 1695.
[21] S. Prag, M. Parsons, M. D. Keppler, S. M. Ameer-Beg, P. Barber, J. Hunt, A. J. Beavil, R. Calvert, M. Arpin, B. Vojnovic, T. Ng, *Mol. Biol. Cell* **2007**, *18*, 2935 – 2948.
[22] F. Zhou, D. Xing, S. Wu, W. R. Chen, *Mol. Imaging Biol.* **2010**, *12*, 63 – 70.
[23] T. Förster, *Ann. Phys.* **1948**, *437*, 55 – 75.
[24] T. Förster in *Modern Quantum Chemistry Part III: Action of LIght and Organic Crystals.* (Ed.: O. Sinanoglu), Academic Press, New York, **1965**, pp. 93 – 137.
[25] L. Stryer, *Annu. Rev. Biochem.* **1978**, *47*, 819 – 846.
[26] Y. L. Wang, *J. Microsc.* **2007**, *228*, 123 – 131.
[27] R. Grailhe, F. Merola, J. Ridard, S. Couvignou, C. L. Poupon, J.-P. Changeux, H. Laguitton-Pasquier, *ChemPhysChem* **2006**, *7*, 1442 – 1454.
[28] O. Pertz, L. Hodgson, R. L. Klemke, K. M. Hahn, *Nature* **2006**, *440*, 1069 – 1072.
[29] M. Machacek, L. Hodgson, C. Welch, H. Elliott, O. Pertz, P. Nalbant, A. Abell, G. L. Johnson, K. M. Hahn, G. Danuser, *Nature* **2009**, *461*, 99 – 103.
[30] Z. Zhou, M. Yu, H. Yang, K. Huang, F. Li, T. Yi, C. Huang, *Chem. Commun.* **2008**, 3387 – 3389.
[31] X. Zhang, Y. Xiao, X. Qian, *Angew. Chem.* **2008**, *120*, 8145 – 8149; *Angew. Chem. Int. Ed.* **2008**, *47*, 8025 – 8029.
[32] A. Miyawaki, J. Llopis, R. Heim, J. M. McCaffery, J. A. Adams, M. Ikura, R. Y. Tsien, *Nature* **1997**, *388*, 882 – 887.
[33] L. M. DiPilato, X. Cheng, J. Zhang, *Proc. Natl. Acad. Sci. USA* **2004**, *101*, 16513 – 16518.
[34] N. Soh, K. Makihara, E. Sakoda, T. Imato, *Chem. Commun.* **2004**, 496 – 497.
[35] A. Piljic, C. Schultz, *ACS Chem. Biol.* **2008**, *3*, 156 – 160.
[36] A. Woehler, J. Wlodarczyk, E. Neher, *Biophys. J.* **2010**, *99*, 2344 – 2354.
[37] D. W. Piston, M. A. Rizzo, *Methods Cell Biol.* **2008**, *85*, 415 – 430.
[38] M. A. Rizzo, D. W. Piston, *Biophys. J.* **2005**, *88*, L14 – 16.
[39] L. M. Carlin, K. Makrogianneli, M. Keppler, G. O. Fruhwirth, T. Ng, *Methods Mol. Biol.* **2010**, *616*, 97 – 113.
[40] K. Makrogianneli, L. M. Carlin, M. D. Keppler, D. R. Matthews, E. Ofo, A. Coolen, S. M. Ameer-Beg, P. R. Barber, B. Vojnovic, T. Ng, *Mol. Cell. Biol.* **2009**, *29*, 2997 – 3006.
[41] M. Beutler, K. Makrogianneli, R. J. Vermeij, M. Keppler, T. Ng, T. M. Jovin, R. Heintzmann, *Eur. Biophys. J.* **2008**, *38*, 69 – 82.
[42] M. T. Kelleher, G. Fruhwirth, G. Patel, E. Ofo, F. Festy, P. R. Barber, S. M. Ameer-Beg, B. Vojnovic, C. Gillett, A. Coolen, G. Keri, P. A. Ellis, T. Ng, *Target Oncol.* **2009**, *4*, 235 – 252.
[43] P. R. Barber, S. M. Ameer-Beg, J. Gilbey, L. M. Carlin, M. Keppler, T. C. Ng, B. Vojnovic, *J. Royal Soc. Interface* **2009**, *6*, S93 – S105.
[44] A. N. Bader, E. G. Hofman, J. Voortman, P. M. P. van Bergen en Henegouwen, H. C. Gerritsen, *Biophys. J.* **2009**, *97*, 2613 – 2622.
[45] I. Gautier, M. Tramier, C. Durieux, J. Coppey, R. B. Pansu, J. C. Nicolas, K. Kemnitz, M. Coppey-Moisan, *Biophys. J.* **2001**, *80*, 3000 – 3008.
[46] M. G. Erickson, D. L. Moon, D. T. Yue, *Biophys. J.* **2003**, *85*, 599 – 611.
[47] S. M. Ameer-Beg, N. Edme, M. Peter, P. R. Barber, T. Ng, B. Vojnovic in *Imaging Protein–Protein Interactions by Multiphoton FLIM, Proc. SPIE* **2003**, *5139*, 180 – 189.
[48] M. Peter, S. M. Ameer-Beg, M. K. Hughes, M. D. Keppler, S. Prag, M. Marsh, B. Vojnovic, T. Ng, *Biophys. J.* **2005**, *88*, 1224 – 1237.
[49] M. K. Y. Hughes, S. M. Ameer-Beg, M. Peter, T. Ng in *Use of Acceptor Fluorescence for Determining FRET Lifetimes, Proc. SPIE* **2003**, *5139*, 88 – 96.
[50] A. Esposito, H. C. Gerritsen, F. S. Wouters, *J. Opt. Soc. Am. A* **2007**, *24*, 3261 – 3273.
[51] F. S. Wouters, A. Esposito, *HFSP J.* **2008**, *2*, 7 – 11.
[52] W. Becker, A. Bergmann, M. Hink, K. König, K. Benndorf, C. Biskup, *Microsc. Res. Tech.* **2004**, *63*, 58 – 66.
[53] P. Barber, S. M. Ameer-beg, S. Pathmananthan, M. Rowley, A. Coolen, *Biomed. Opt. Expr.* **2010**, *1*, 1148 – 1158.
[54] H. C. Gerritsen, M. A. Asselbergs, A. V. Agronskaia, W. G. Van Sark, *J. Microsc.* **2002**, *206*, 218 – 224.
[55] A. Elder, S. Schlachter, C. F. Kaminski, *J. Opt. Soc. Am. A* **2008**, *25*, 452 – 462.
[56] E. A. Jares-Erijman, T. M. Jovin, *Nat. Biotechnol.* **2003**, *21*, 1387 – 1395.
[57] E. A. Jares-Erijman, T. M. Jovin, *Curr. Opin. Chem. Biol.* **2006**, *10*, 409 – 416.
[58] G. N. van der Krogt, J. Ogink, B. Ponsioen, K. Jalink, *PLoS One* **2008**, *3*, e1916.
[59] L. Albertazzi, D. Arosio, L. Marchetti, F. Ricci, F. Beltram, *Photochem. Photobiol.* **2009**, *85*, 287 – 297.
[60] N. C. Shaner, R. E. Campbell, P. A. Steinbach, B. N. Giepmans, A. E. Palmer, R. Y. Tsien, *Nat. Biotechnol.* **2004**, *22*, 1567 – 1572.
[61] T. Holbro, R. R. Beerli, F. Maurer, M. Koziczak, C. F. Barbas III, N. E. Hynes, *Proc. Natl. Acad. Sci. USA* **2003**, *100*, 8933 – 8938.
[62] E. M. Merzlyak, J. Goedhart, D. Shcherbo, M. E. Bulina, A. S. Shcheglov, A. F. Fradkov, A. Gaintzeva, K. A. Lukyanov, S. Lukyanov, T. W. J. Gadella, D. M. Chudakov, *Nat. Methods* **2007**, *4*, 555 – 557.
[63] H.-w. Ai, K. L. Hazelwood, M. W. Davidson, R. E. Campbell, *Nat. Methods* **2008**, *5*, 401 – 403.
[64] W. Tomosugi, T. Matsuda, T. Tani, T. Nemoto, I. Kotera, K. Saito, K. Horikawa, T. Nagai, *Nat. Methods* **2009**, *6*, 351 – 353.
[65] S. Ganesan, S. M. Ameer-beg, T. Ng, B. Vojnovic, F. S. Wouters, *Proc. Natl. Acad. Sci. USA* **2006**, *103*, 4089 – 4094.
[66] X. Shu, A. Royant, M. Z. Lin, T. A. Aguilera, V. Lev-Ram, P. A. Steinbach, R. Y. Tsien, *Science* **2009**, *324*, 804 – 807.
[67] M. Köllner, J. Wolfrum, *Chem. Phys. Lett.* **1992**, *200*, 199 – 204.
[68] S. Shimozono, H. Hosoi, H. Mizuno, T. Fukano, T. Tahara, A. Miyawaki, *Biochemistry* **2006**, *45*, 6267 – 6271.
[69] M. A. Digman, V. R. Caiolfa, M. Zamai, E. Gratton, *Biophys. J.* **2008**, *94*, L14 – L16.
[70] T. Ng, A. Squire, G. Hansra, F. Bornancin, C. Prevostel, A. Hanby, W. Harris, D. Barnes, S. Schmidt, H. Mellor, P. I. Bastiaens, P. J. Parker, *Science* **1999**, *283*, 2085 – 2089.
[71] T. Ng, D. Shima, A. Squire, P. I. H. Bastiaens, S. Gschmeissner, M. J. Humphries, P. J. Parker, *EMBO J.* **1999**, *18*, 3909 – 3923.
[72] C. Hoffmann, G. Gaietta, M. Bunemann, S. R. Adams, S. Oberdorff-Maass, B. Behr, J. P. Vilardaga, R. Y. Tsien, M. H. Ellisman, M. J. Lohse, *Nat. Methods* **2005**, *2*, 171 – 176.
[73] D. Maurel, L. Comps-Agrar, C. Brock, M.-L. Rives, E. Bourrier, M. A. Ayoub, H. Bazin, N. Tinel, T. Durroux, L. Prezeau, E. Trinquet, J.-P. Pin, *Nat. Methods* **2008**, *5*, 561 – 567.
[74] A. Gautier, A. Juillerat, C. Heinis, I. R. Corrêa, M. Kindermann, F. Beaufils, K. Johnsson, *Chem. Biol.* **2008**, *15*, 128 – 136.
[75] M. Parsons, T. Ng, *Method Cell Biol.* **2002**, *69*, 261 – 278.
[76] D. Steiner, P. Forrer, A. Pluckthun, *J. Mol. Biol.* **2008**, *382*, 1211 – 1227.
[77] Y. C. Chuan, S. T. Pang, A. Cedazo-Minguez, G. Norstedt, A. Pousette, A. Flores-Morales, *J. Biol. Chem.* **2006**, *281*, 29938 – 29948.
[78] C. Khanna, X. Wan, S. Bose, R. Cassaday, O. Olomu, A. Mendoza, C. Yeung, R. Gorlick, S. M. Hewitt, L. J. Helman, *Nat. Med.* **2004**, *10*, 182 – 186.
[79] Y. Yu, J. Khan, C. Khanna, L. Helman, P. S. Meltzer, G. Merlino, *Nat. Med.* **2004**, *10*, 175 – 181.
[80] B. E. Elliott, J. A. Meens, S. K. SenGupta, D. Louvard, M. Arpin, *Breast Cancer Res.* **2005**, *7*, R365 – 373.
[81] H. Erfle, B. Neumann, U. Liebel, P. Rogers, M. Held, T. Walter, J. Ellenberg, R. Pepperkok, *Nat. Protoc.* **2007**, *2*, 392 – 399.
[82] B. Neumann, M. Held, U. Liebel, H. Erfle, P. Rogers, R. Pepperkok, J. Ellenberg, *Nat. Methods* **2006**, *3*, 385 – 390.
[83] D. Matallanas, D. Romano, K. Yee, K. Meissl, L. Kucerova, D. Piazzolla, M. Baccarini, J. K. Vass, W. Kolch, E. O'Neill, *Mol. Cell* **2007**, *27*, 962 – 975.
[84] E. O'Neill, W. Kolch, *Cell Cycle* **2005**, *4*, 365 – 367.
[85] E. O'Neill, L. Rushworth, M. Baccarini, W. Kolch, *Science* **2004**, *306*, 2267 – 2270.
[86] D. Romano, D. Matallanas, G. Weitsman, C. Preisinger, T. Ng, W. Kolch, *Cancer Res.* **2010**, *70*, 1195 – 1203.
[87] N. Juul, Z. Szallasi, A. C. Eklund, Q. Li, R. A. Burrell, M. Gerlinger, V. Valero, E. Andreopoulou, F. J. Esteva, W. F. Symmans, C. Desmedt, B. Haibe-Kains, C. Sotiriou, L. Pusztai, C. Swanton, *Lancet Oncol.* **2010**, *11*, 358 – 365.
[88] C. Sotiriou, L. Pusztai, *New Engl. J. Med.* **2009**, *360*, 790 – 800.
[89] A. Platzer, P. Perco, A. Lukas, B. Mayer, *BMC Bioinf.* **2007**, *8*, 224.

  

[90] G. O. Fruhwirth, S. Ameer-Beg, R. Cook, T. Watson, T. Ng, F. Festy, *Opt. Express* **2010**, *18*, 11148 – 11158.
[91] G. Fruhwirth, D. R. Matthews, A. Brock, M. Keppler, B. Vojnovic, T. Ng, S. M. Ameer-Beg in *Deep-Tissue Multiphoton Fluorescence Lifetime Microscopy for Intravital Imaging of Protein–Protein Interactions, Proc. SPIE* **2009**, *7183*, 71 830 – 71 839.
[92] E. M. Bublil, G. Pines, G. Patel, G. Fruhwirth, T. Ng, Y. Yarden, *FASEB J.* **2010**, *24*, 4744 – 4755.
[93] N. I. Cade, G. Fruhwirth, S. J. Archibald, T. Ng, D. Richards, *Biophys. J.* **2010**, *98*, 2752 – 2757.
[94] G. Tarcic, S. K. Boguslavsky, J. Wakim, T. Kiuchi, A. Liu, F. Reinitz, D. Nathanson, T. Takahashi, P. S. Mischel, T. Ng, Y. Yarden, *Curr. Biol.* **2009**, *19*, 1788 – 1798.
[95] P. Konig, G. Krasteva, C. Tag, I. R. Konig, C. Arens, W. Kummer, *Lab. Invest.* **2006**, *86*, 853 – 864.
[96] S. Dadke, S. Cotteret, S. C. Yip, Z. M. Jaffer, F. Haj, A. Ivanov, F. Rauscher III, K. Shuai, T. Ng, B. G. Neel, J. Chernoff, *Nat. Cell Biol.* **2007**, *9*, 80 – 85.
[97] J. R. Morris, C. Boutell, M. Keppler, R. Densham, D. Weekes, A. Alamshah, L. Butler, Y. Galanty, L. Pangon, T. Kiuchi, T. Ng, E. Solomon, *Nature* **2009**, *462*, 886 – 890.
[98] P. Nalbant, L. Hodgson, V. Kraynov, A. Toutchkine, K. M. Hahn, *Science* **2004**, *305*, 1615 – 1619.
[99] O. Pertz, K. M. Hahn, *J. Cell Sci.* **2004**, *117*, 1313 – 1318.
[100] M. A. Del Pozo, W. B. Kiosses, N. B. Alderson, N. Meller, K. M. Hahn, M. A. Schwartz, *Nat. Cell Biol.* **2002**, *4*, 232 – 239.
[101] P. Niethammer, P. Bastiaens, E. Karsenti, *Science* **2004**, *303*, 1862 – 1866.
[102] M. Keese, R. J. Magdeburg, T. Herzog, T. Hasenberg, M. Offterdinger, R. Pepperkok, J. W. Sturm, P. I. Bastiaens, *J. Biol. Chem.* **2005**, *280*, 27826 – 27831.
[103] A. Kong, P. Leboucher, R. Leek, V. Calleja, S. Winter, A. Harris, P. J. Parker, B. Larijani, *Cancer Res.* **2006**, *66*, 2834 – 2843.
[104] S. A. Lee, C. H. Chan, T. C. Chen, C. Y. Yang, K. C. Huang, C. H. Tsai, J. M. Lai, F. S. Wang, C. Y. Kao, C. Y. Huang, *BMC Bioinf.* **2009**, *10*, 114.
[105] Y. R. Cho, W. Hwang, M. Ramanathan, A. Zhang, *BMC Bioinf.* **2007**, *8*, 265.
[106] M. T. Dittrich, G. W. Klau, A. Rosenwald, T. Dandekar, T. Muller, *Bioinformatics* **2008**, *24*, i223 – 231.
[107] E. Georgii, S. Dietmann, T. Uno, P. Pagel, K. Tsuda, *Bioinformatics* **2009**, *25*, 933 – 940.
[108] H. Ritter, T. Martinetz, K. Schulten, *Neural Computation and Self-Organizing Maps*, Addison-Wesley, New York, **1992**.
[109] P. Tamayo, D. Slonim, J. Mesirov, Q. Zhu, S. Kitareewan, E. Dmitrovsky, E. S. Lander, T. R. Golub, *Proc. Natl. Acad. Sci. USA* **1999**, *96*, 2907 – 2912.
[110] S. Bloch, F. Lesage, L. McIntosh, A. Gandjbakhche, K. Liang, S. Achilefu, *J. Biomed. Opt.* **2005**, *10*, 054003.
[111] A. T. N. Kumar, S. B. Raymond, A. K. Dunn, B. J. Bacskai, D. A. Boas, *IEEE Trans. Med. Imaging* **2008**, *27*, 1152 – 1163.
[112] A. T. N. Kumar, E. Chung, S. B. Raymond, J. A. J. M. Van De Water, K. Shah, D. Fukumura, R. K. Jain, B. J. Bacskai, D. A. Boas, *Opt. Lett.* **2009**, *34*, 2066 – 2068.
[113] J. Sharpe, U. Ahlgren, P. Perry, B. Hill, A. Ross, J. Hecksher-Sorensen, R. Baldock, D. Davidson, *Science* **2002**, *296*, 541 – 545.
[114] N. Deliolanis, T. Lasser, D. Hyde, A. Soubret, J. Ripoll, V. Ntziachristos, *Opt. Lett.* **2007**, *32*, 382 – 384.
[115] J. McGinty, V. Y. Soloviev, K. B. Tahir, R. Laine, D. W. Stuckey, J. V. Hajnal, A. Sardini, P. M. French, S. R. Arridge, *Opt. Lett.* **2009**, *34*, 2772 – 2774.
[116] G. M. Turner, G. Zacharakis, A. Soubret, J. Ripoll, V. Ntziachristos, *Opt. Lett.* **2005**, *30*, 409 – 411.
[117] P. Friedl, D. Gilmour, *Nat. Rev.* **2009**, *10*, 445 – 457.
[118] E. Sahai, *Nat. Rev. Cancer* **2007**, *7*, 737 – 749.
[119] W. Wang, S. Goswami, K. Lapidus, A. L. Wells, J. B. Wyckoff, E. Sahai, R. H. Singer, J. E. Segall, J. S. Condeelis, *Cancer Res.* **2004**, *64*, 8585 – 8594.
[120] J. B. Wyckoff, S. E. Pinner, S. Gschmeissner, J. S. Condeelis, E. Sahai, *Curr. Biol.* **2006**, *16*, 1515 – 1523.
[121] M. Canel, A. Serrels, D. Miller, P. Timpson, B. Serrels, M. C. Frame, V. G. Brunton, *Cancer Res.* **2010**, *70*, 9413 – 9422.
[122] D. Kedrin, B. Gligorijevic, J. Wyckoff, V. V. Verkhusha, J. Condeelis, J. E. Segall, J. van Rheenen, *Nat. Methods* **2008**, *5*, 1019 – 1021.
[123] B. Gligorijevic, D. Kedrin, J. E. Segall, J. Condeelis, J. van Rheenen, *J. Vis. Exp.* **2008**, *5*, 1019 – 1021.
[124] J. Condeelis, R. Weissleder, *Cold Spring Harbour Perspect. Biol.* **2010**, *2*, a003848.
[125] F. Helmchen, W. Denk, *Nat. Methods* **2005**, *2*, 932 – 940.
[126] J. M. Girkin, S. Poland, A. J. Wright, *Curr. Opin. Biotechnol.* **2009**, *20*, 106 – 110.
[127] R. K. Tyson in *Principles of Adaptive Optics*, Academic Press, Boca Raton, **1997**.
[128] M. J. Booth, M. A. Neil, R. Juskaitis, T. Wilson, *Proc. Natl. Acad. Sci. USA* **2002**, *99*, 5788 – 5792.
[129] P. Marsh, D. Burns, J. Girkin, *Opt. Express* **2003**, *11*, 1123 – 1130.
[130] A. J. Wright, S. P. Poland, J. M. Girkin, C. W. Freudiger, C. L. Evans, X. S. Xie, *Opt. Express* **2007**, *15*, 18209 – 18219.
[131] A. Jesacher, A. Thayil, K. Grieve, D. Debarre, T. Watanabe, T. Wilson, S. Srinivas, M. Booth, *Opt. Lett.* **2009**, *34*, 3154 – 3156.
[132] N. Ji, D. E. Milkie, E. Betzig, *Nat. Methods* **2010**, *7*, 141 – 147.
[133] F. Festy, S. M. Ameer-Beg, T. Ng, K. Suhling, *Mol. Biosyst.* **2007**, *3*, 381 – 391.
[134] F. S. Wouters, P. J. Verveer, P. I. Bastiaens, *Trends Cell Biol.* **2001**, *11*, 203 – 211.
[135] J. L. Vinkenborg, T. J. Nicolson, E. A. Bellomo, M. S. Koay, G. A. Rutter, M. Merkx, *Nat. Methods* **2009**, *6*, 737 – 740.
[136] A. E. Palmer, M. Giacomello, T. Kortemme, S. A. Hires, V. Lev-Ram, D. Baker, R. Y. Tsien, *Chem. Biol.* **2006**, *13*, 521 – 530.
[137] A. W. Nguyen, P. S. Daugherty, *Nat. Biotechnol.* **2005**, *23*, 355 – 360.
[138] C. W. Lin, A. Y. Ting, *Angew. Chem.* **2004**, *116*, 3000 – 3003; *Angew. Chem. Int. Ed.* **2004**, *43*, 2940 – 2943.
[139] V. O. Nikolaev, S. Gambaryan, M. J. Lohse, *Nat. Methods* **2006**, *3*, 23 – 25.
[140] A. E. Palmer, R. Y. Tsien, *Nat. Protoc.* **2006**, *1*, 1057 – 1065.
[141] T. Nakamura, K. Aoki, M. Matsuda, *Methods* **2005**, *37*, 146 – 153.
[142] A. Esposito, M. Gralle, M. A. Dani, D. Lange, F. S. Wouters, *Biochemistry* **2008**, *47*, 13115 – 13126.
[143] H. W. Ai, J. N. Henderson, S. J. Remington, R. E. Campbell, *Biochem. J.* **2006**, *400*, 531 – 540.
[144] J. Goedhart, L. van Weeren, M. A. Hink, N. O. E. Vischer, K. Jalink, T. W. J. Gadella, *Nat. Methods* **2010**, *7*, 137 – 139.
[145] V. Bayle, L. Nussaume, R. A. Bhat, *Plant Physiol.* **2008**, *148*, 51 – 60.
[146] H. Tsutsui, S. Karasawa, Y. Okamura, A. Miyawaki, *Nat. Methods* **2008**, *5*, 683 – 685.
[147] S. Karasawa, T. Araki, T. Nagai, H. Mizuno, A. Miyawaki, *Biochem. J.* **2004**, *381*, 307 – 312.
[148] D. Llères, J. James, S. Swift, D. G. Norman, A. I. Lamond, *J. Cell Biol.* **2009**, *187*, 481 – 496.
[149] S. Ebbinghaus, A. Dhar, J. D. McDonald, M. Gruebele, *Nat .Methods* **2010**, *7*, 319 – 323.
[150] D. Shcherbo, E. A. Souslova, J. Goedhart, T. V. Chepurnykh, A. Gaintzeva, Shemiakina II, T. W. Gadella, S. Lukyanov, D. M. Chudakov, *BMC Biotechnol.* **2009**, *9*, 24.
[151] S. Harbaugh, N. Kelley-Loughnane, M. Davidson, L. Narayanan, S. Trott, Y. G. Chushak, M. O. Stone, *Biomacromolecules* **2009**, *10*, 1055 – 1060.
[152] J. Goedhart, J. E. M. Vermeer, M. J. W. Adjobo-Hermans, L. van Weeren, T. W. J. Gadella, Jr., *PLoS One* **2007**, *2*, e1011.
[153] Z. N. Ba'no'czi, A. Alexa, A. Farkas, P. T. Friedrich, F. Hudecz, *Bioconjugate Chem.* **2008**, *19*, 1375 – 1381.
[154] A. Kuznetsov, V. P. Bindokas, J. D. Marks, L. H. Philipson, *Am. J. Physiol.* **2005**, *289*, C224 – C229.
[155] R. B. Thompson, R. Bozym, M. L. Cramer, A. K. Stoddard, N. M. Westerberg, C. A. Fierke in *Carbonic Anhydrase-Based Biosensing of Metal Ions: Issues and Future Prospects* (Ed.: R. B. Thompson), CRC, Boca Raton, **2005**, pp. 107 – 117.
[156] R. B. Thompson, M. L. Cramer, R. Bozym, C. A. Fierke, *J. Biomed. Opt.* **2002**, *7*, 555 – 560.
[157] C. A. Jost, G. Reither, C. Hoffmann, C. Schultz, *ChemBioChem* **2008**, *9*, 1379 – 1384.
[158] J. Nakanishi, T. Takarada, S. Yunoki, Y. Kikuchi, M. Maeda, *Biochem. Biophys. Res. Commun.* **2006**, *343*, 1191 – 1196.
[159] H. M. Watrob, C.-P. Pan, M. D. Barkley, *J. Am. Chem. Soc.* **2003**, *125*, 7336 – 7343.


  

[160] L. Albizu, M. Cottet, M. Kralikova, S. Stoev, R. Seyer, I. Brabet, T. Roux, H. Bazin, E. Bourrier, L. Lamarque, C. Breton, M.-L. Rives, A. Newman, J. Javitch, E. Trinquet, M. Manning, J.-P. Pin, B. Mouillac, T. Durroux, *Nat. Chem. Biol.* **2010**, *6*, 587 – 594.
[161] M. J. Hangauer, C. R. Bertozzi, *Angew. Chem.* **2008**, *120*, 2428 – 2431; *Angew. Chem. Int. Ed.* **2008**, *47*, 2394 – 2397.
[162] S. Jin, F. Yi, F. Zhang, J. L. Poklis, P. L. Li, *Arterioscler. Thromb. Vasc. Biol.* **2008**, *28*, 2056 – 2062.
[163] A. H. A. Clayton, F. Walker, S. G. Orchard, C. Henderson, D. Fuchs, J. Rothacker, E. C. Nice, A. W. Burgess, *J. Biol. Chem.* **2005**, *280*, 30392 – 30399.
[164] A. H. A. Clayton, M. L. Tavarnesi, T. G. Johns, *Biochemistry* **2007**, *46*, 4589 – 4597.
[165] S.-H. Hong, W. Maret, *Proc. Natl. Acad. Sci. USA* **2003**, *100*, 2255 – 2260.
[166] M. J. Roberti, C. W. Bertoncini, R. Klement, E. A. Jares-Erijman, T. M. Jovin, *Nat. Methods* **2007**, *4*, 345 – 351.
[167] K. Plafker, I. G. Macara, *J. Biol. Chem.* **2002**, *277*, 30121 – 30127.
[168] A. Luciani, V. R. Villella, A. Vasaturo, I. Giardino, V. Raia, M. Pettoello-Mantovani, M. D'Apolito, S. Guido, T. Leal, S. Quaratino, L. Maiuri, *J. Immunol.* **2009**, *183*, 2775 – 2784.
[169] A. K. Kenworthy, *Methods* **2001**, *24*, 289 – 296.
[170] M. Ogawa, N. Kosaka, P. L. Choyke, H. Kobayashi, *Bioconjugate Chem.* **2009**, *20*, 147 – 154.
[171] E. Rusinova, V. Tretyachenko-Ladokhina, O. E. Vele, D. F. Senear, J. B. Alexander Ross, *Anal. Biochem.* **2002**, *308*, 18 – 25.
[172] P. Sarkar, S. Sridharan, R. Luchowski, S. Desai, B. Dworecki, M. Nlend, Z. Gryczynski, I. Gryczynski, *J. Photochem. Photobiol. B* **2010**, *98*, 35 – 39.
[173] J. van der Greef, R. N. McBurney, *Nat. Rev. Drug Discov.* **2005**, *4*, 961 – 967.
[174] H. Y. Chuang, E. Lee, Y. T. Liu, D. Lee, T. Ideker, *Mol. Syst. Biol.* **2007**, *3*, 140.
[175] N. D. Lawrence, *J. Machine Learning Res.* **2005**, *6*, 1783 – 1816.

Received: October 14, 2010
Revised: January 7, 2011
Published online on February 15, 2011

  

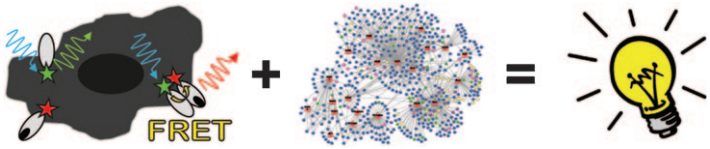


**Worth more than a thousand words:** FRET imaging can contribute at various stages to delineate the function of the proteome. We describe the basic principles of FRET imaging and discuss advanced high-content and intravital FRET imaging techniques with a special focus on their integration with protein interaction networks (see graphic).

*G. O. Fruhwirth,* L. P. Fernandes, G. Weitsman, G. Patel, M. Kelleher, K. Lawler, A. Brock, S. P. Poland, D. R. Matthews, G. Keri, P. R. Barber, B. Vojnovic, S. M. Ameer-Beg, A. C. C. Coolen, F. Fraternali, T. Ng**

■■ – ■■

**How Förster Resonance Energy Transfer Imaging Improves the Understanding of Protein Interaction Networks in Cancer Biology**

  